May 22nd, 2023, Tokyo

2nd Workshop on Hadron Interactions, Hyper-Nuclei and Exotic Hadron productions at High-Energy Experiments

Recent Light Hypernuclei Measurements from STAR Experiment

Xiujun Li

University of Science and Technology of China

University of Tsukuba

Outline

- Introduction
- Review of previous hypernuclei measurements from STAR
- Recent results of hypernuclei from STAR
    - Internal structure
        - Branching ratios, lifetimes, Λ binding energies
    - Production mechanism in heavy-ion collisions
        - Yields, collectivity
    - Discovery of $^{4}_{\Lambda}\overline{\mathrm{H}}$
- Summary
- Outlook

Introduction: what and why

- What are hypernuclei?
  - Bound nuclear systems of non-strange and strange baryons

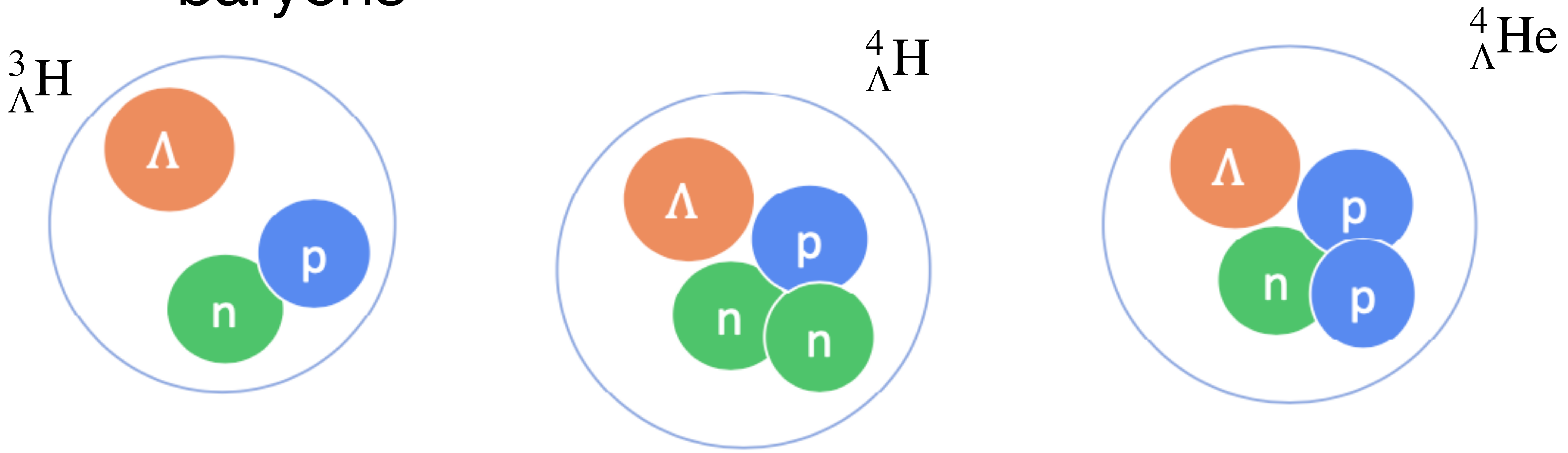

Marian Danysz (right) and Jerzy Pniewski (left) discovered hypernuclei in 1952

- Why hypernuclei?
  - Probe hyperon-nucleon (Y-N) interaction
  - Strangeness in high density nuclear matter
    - Equation-of-State (EoS) of neutron star

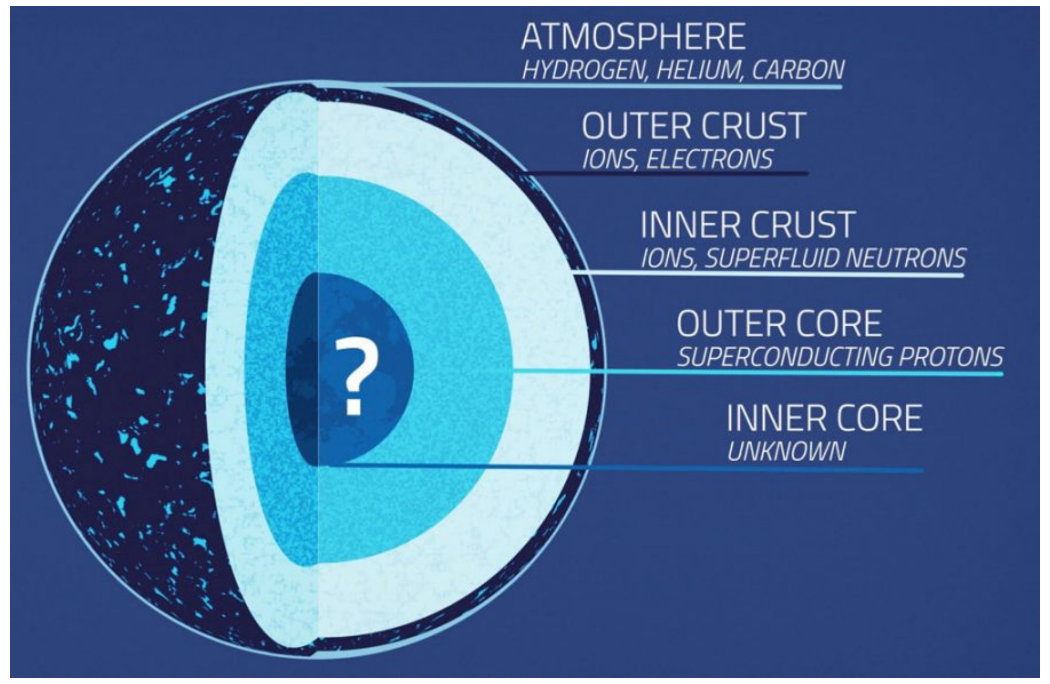

neutron star

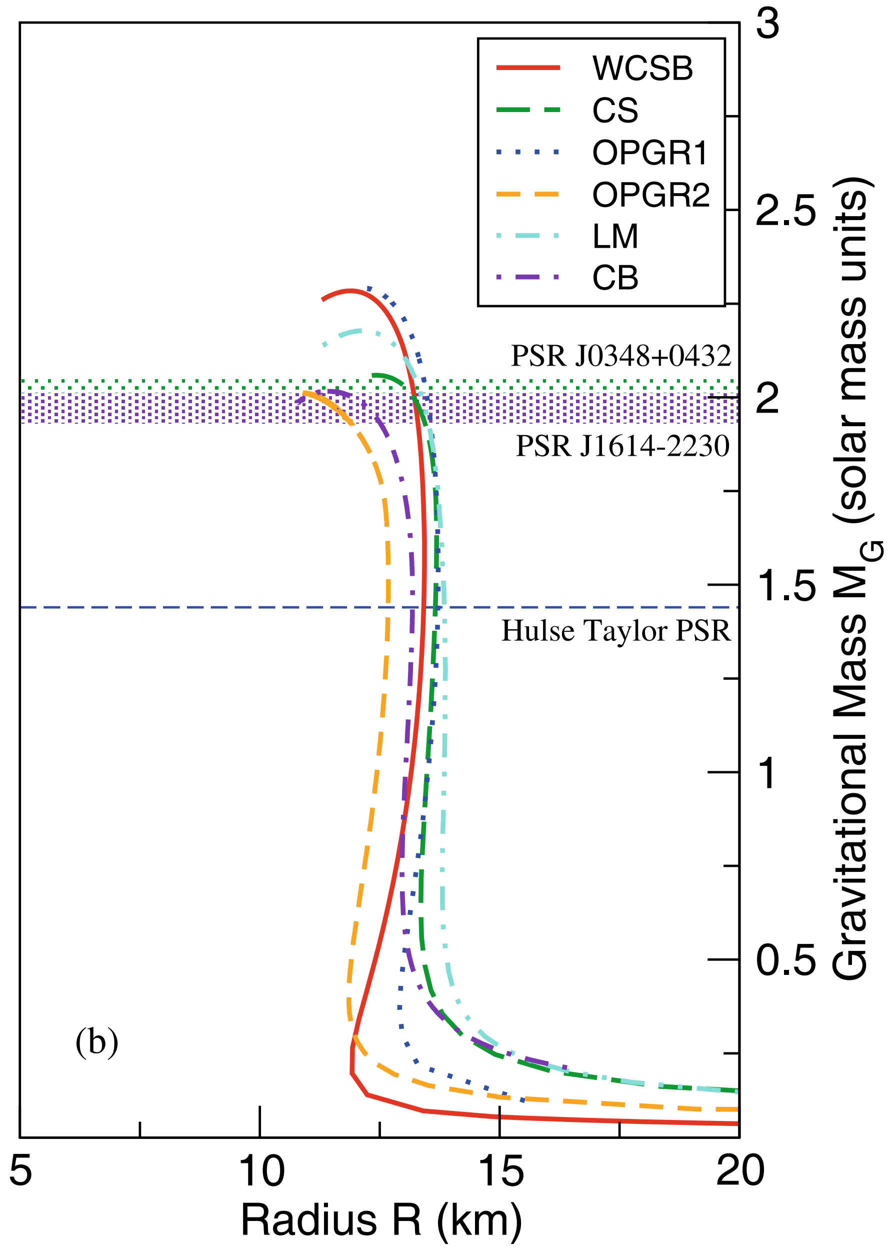

D. Chatterjee, Eur. Phys. J. A (2016) 52: 29

Introduction: how

- Experimentally, we can make measurements related to:

1. Internal structure
    - Lifetime, binding energy, branching ratios etc.

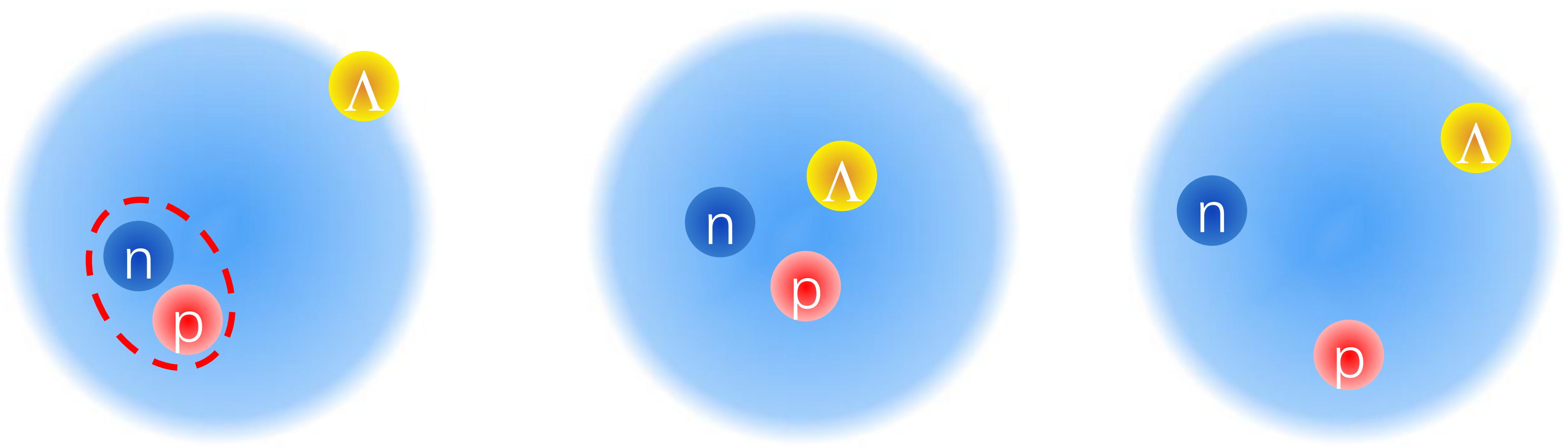

Understanding hypernuclei structure can provide insights to the Y-N interaction

2. Production mechanism
    - Spectra, collectivity etc.

The process of hypernuclei formation in violent heavy-ion collisions is not well understood

Introduction: RHIC BES program

- During the BES-II program, STAR utilized the fixed-target (FXT) setup, which extends the energy reach below $\sqrt{s_{NN}}$ = 7.7 GeV, down to 3.0 GeV

FXT mode setup of STAR detector :

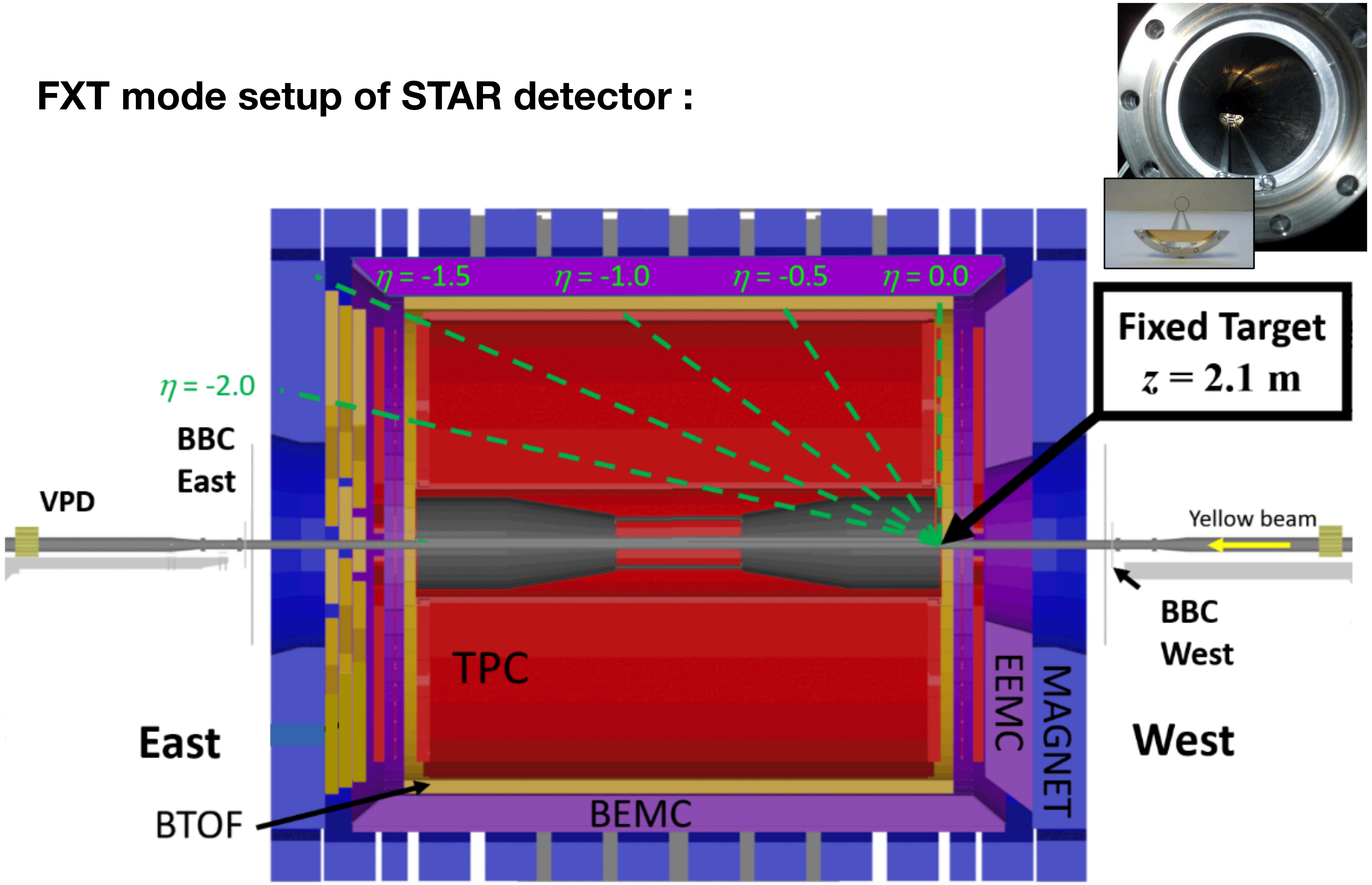

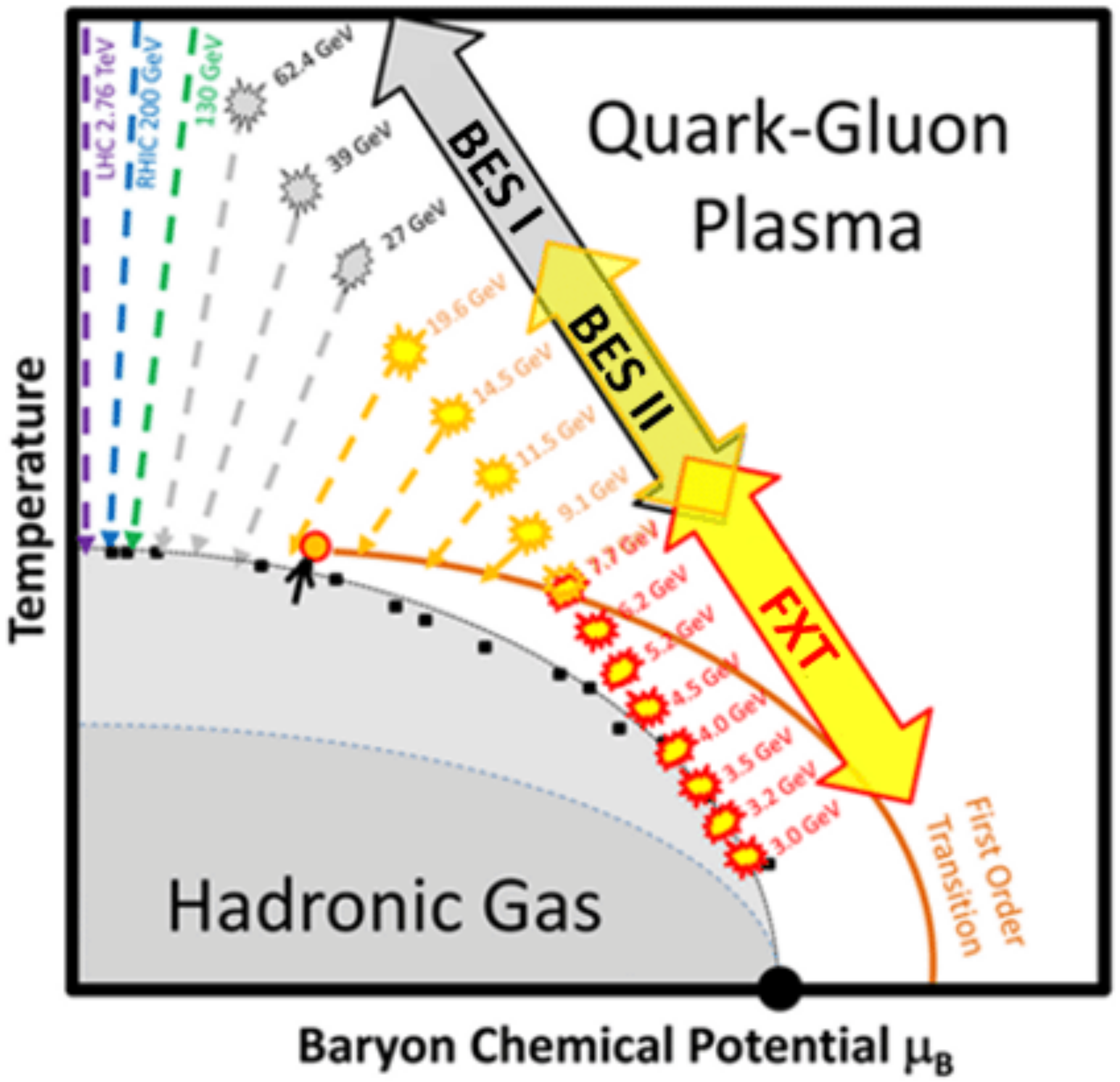

Hypernuclei and STAR BES-II

- **Hypernuclei measurements are scarce in heavy-ion collision experiments**

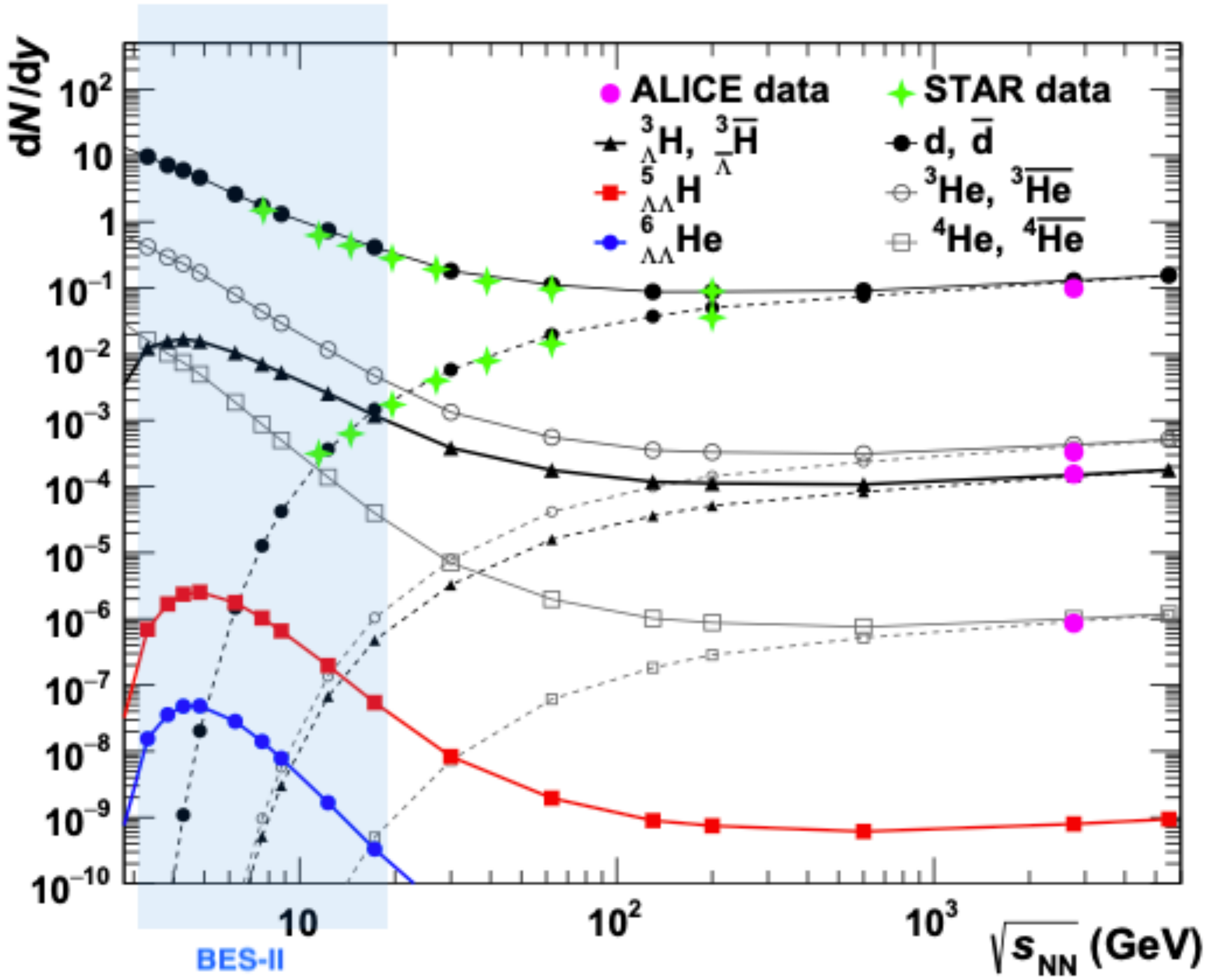

B. Dönigus, Eur. Phys. J. A (2020) 56:280
A. Andronic et al. PLB (2011) 697:203–207

- At low beam energies, hypernuclei production is expected to be enhanced due to high baryon density
- Datasets with large statistics taken during BES-II

→ A great opportunity to study hypernuclei production

List of BES-II datasets:

Year	$\sqrt{s_{NN}}$ [GeV]	Events
2018	27	555 M
	3.0	258 M
	7.2	155 M
2019	19.6	478 M
	14.6	324 M
	3.9	53 M
	3.2	201 M
	7.7	51 M
2020	11.5	235 M
	7.7	113 M
	4.5	108 M
	6.2	118 M
	5.2	103 M
	3.9	117 M
	3.5	116 M
	9.2	162 M
	7.2	317 M
2021	7.7	101 M
	3.0	2103 M
	9.2	54 M
	11.5	52 M
	13.7	51 M
	17.3	256 M
	7.2	89 M

Previous hypernuclei measurements from STAR

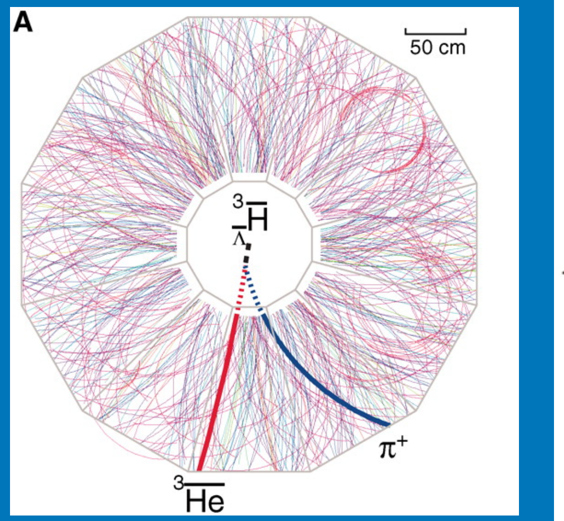

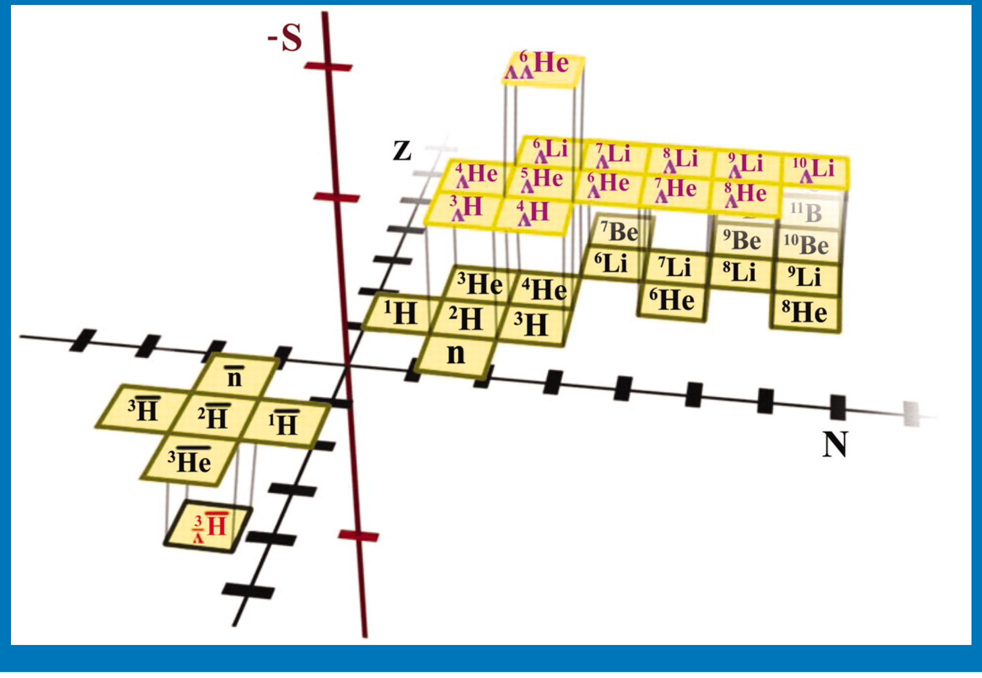

STAR collaboration **made the discovery of the anti-hyper triton.**

Science 328, 58 (2010) (STAR)

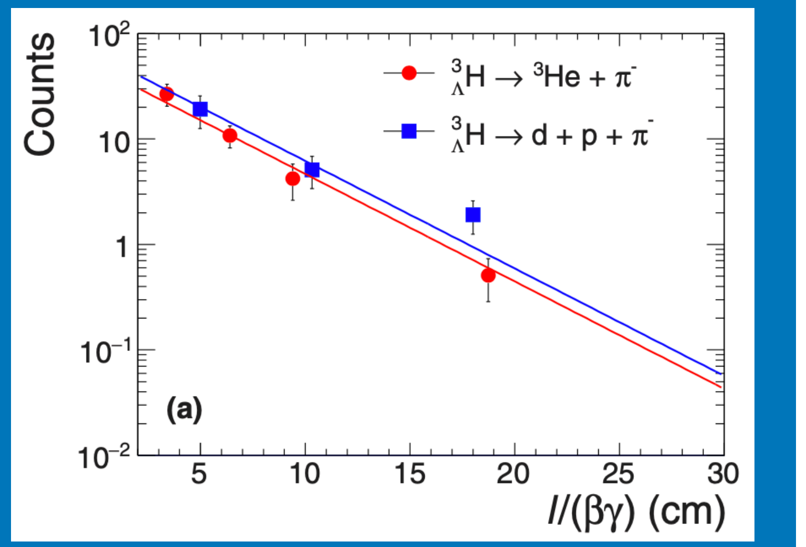

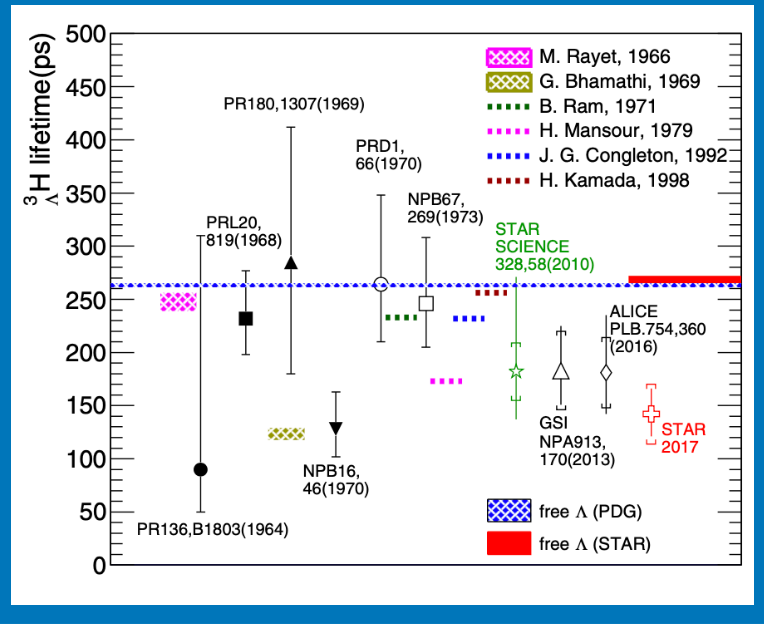

Lifetime measurement of $^{3}_{\Lambda}\mathrm{H}$

Science 328, 58 (2010) (STAR)

PRC 97, 054909 (2018) (STAR)

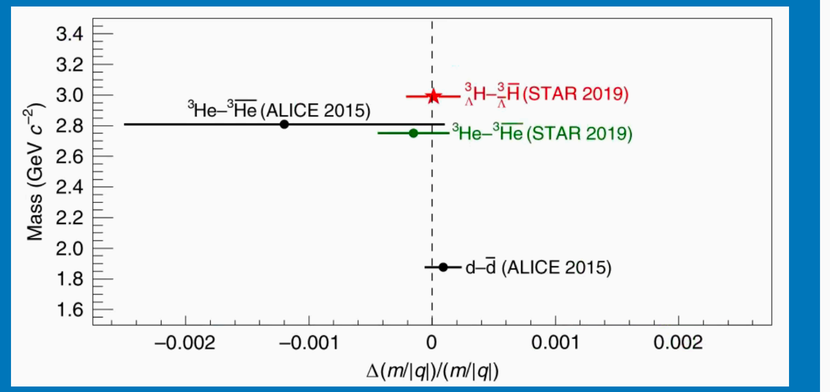

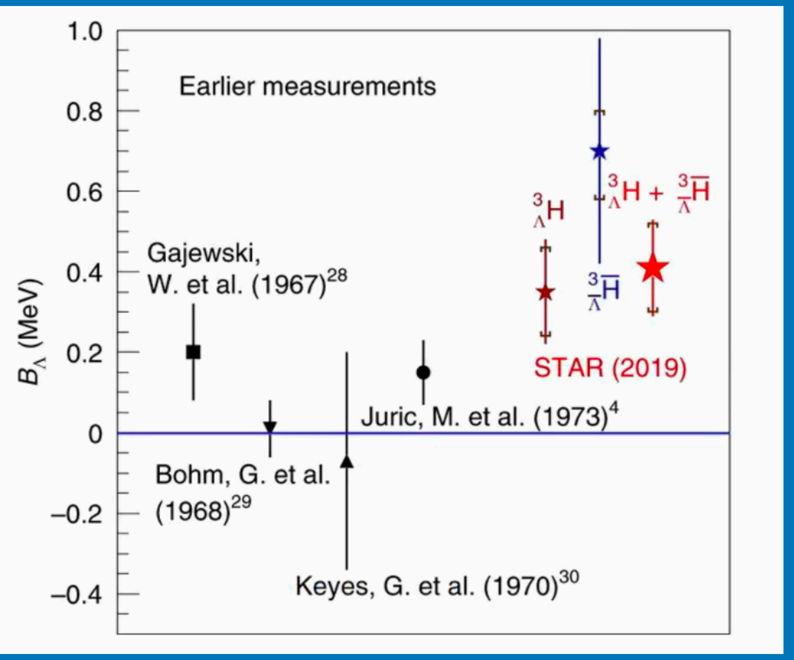

Measurement of mass difference and binding energies of $^{3}_{\Lambda}\mathrm{H}$ and $^{3}_{\bar{\Lambda}}\overline{\mathrm{H}}$

Nature Phys. 16 (2020) 409 (STAR)

Particle identification and hypernuclei reconstruction

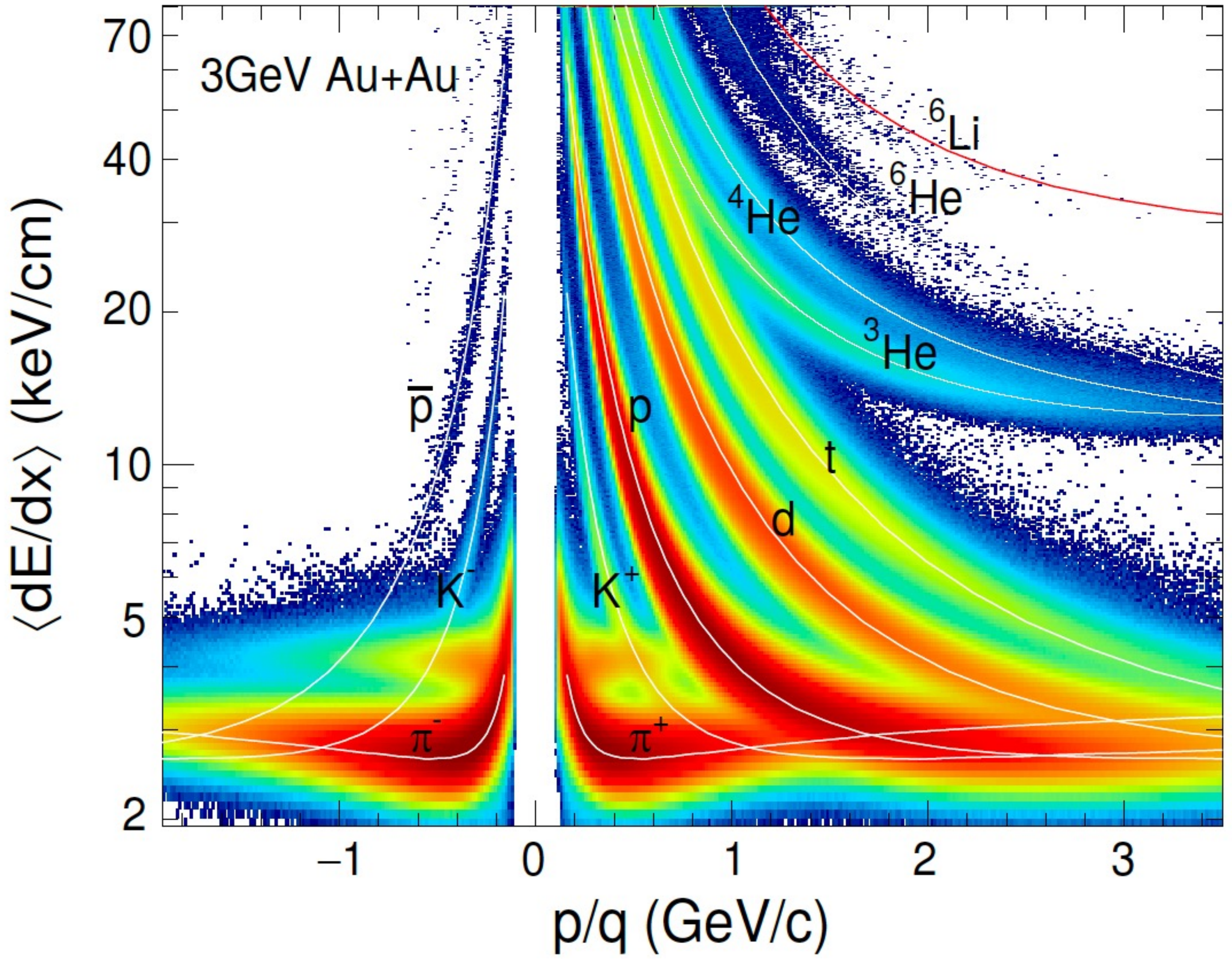

$^{3}_{\Lambda}\mathrm{H} \rightarrow \mathrm{d} + \mathrm{p} + \pi^{-}$:

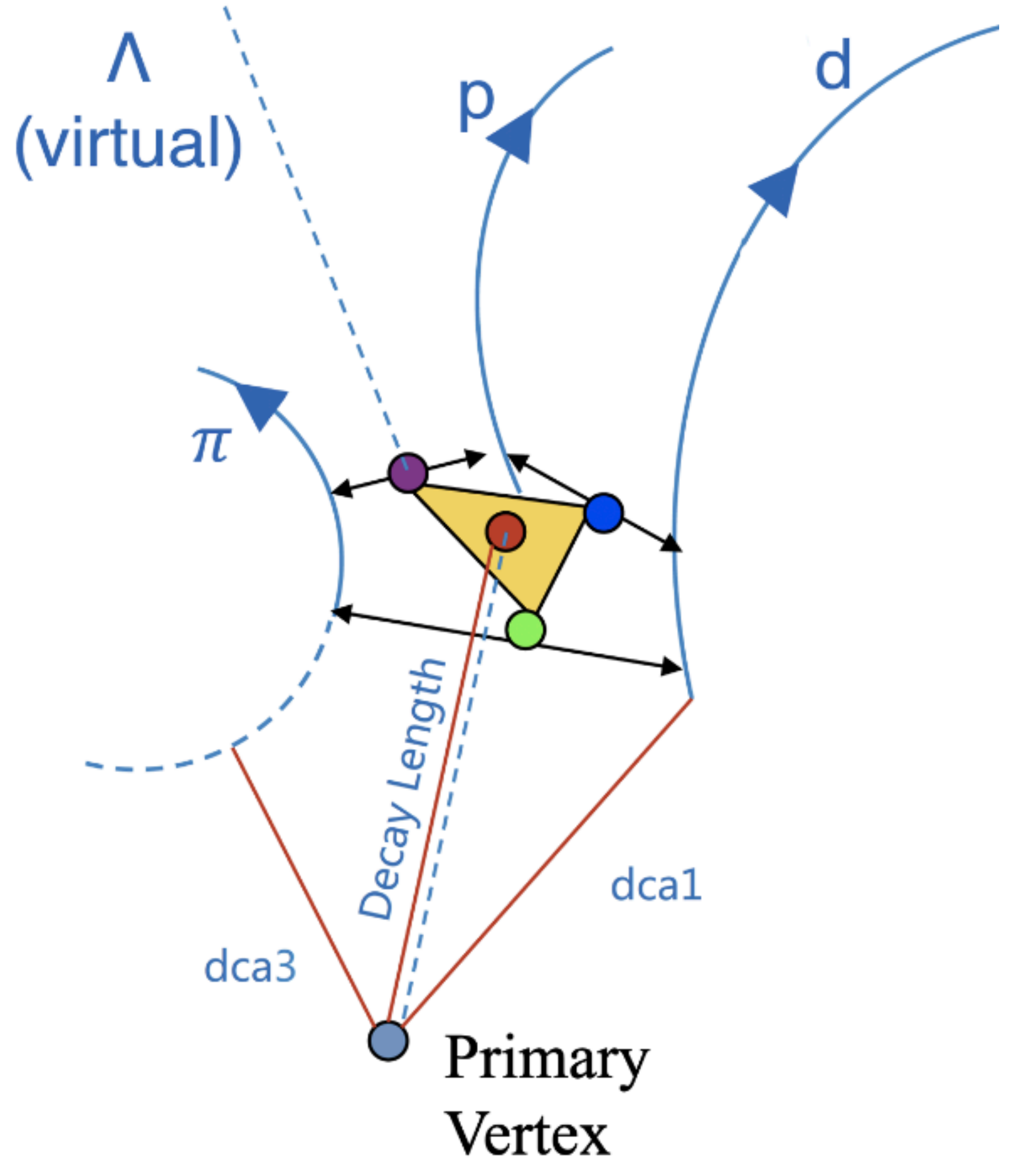

$^{3}_{\Lambda}\mathrm{H} \rightarrow {}^{3}\mathrm{He} + \pi^{-}$:

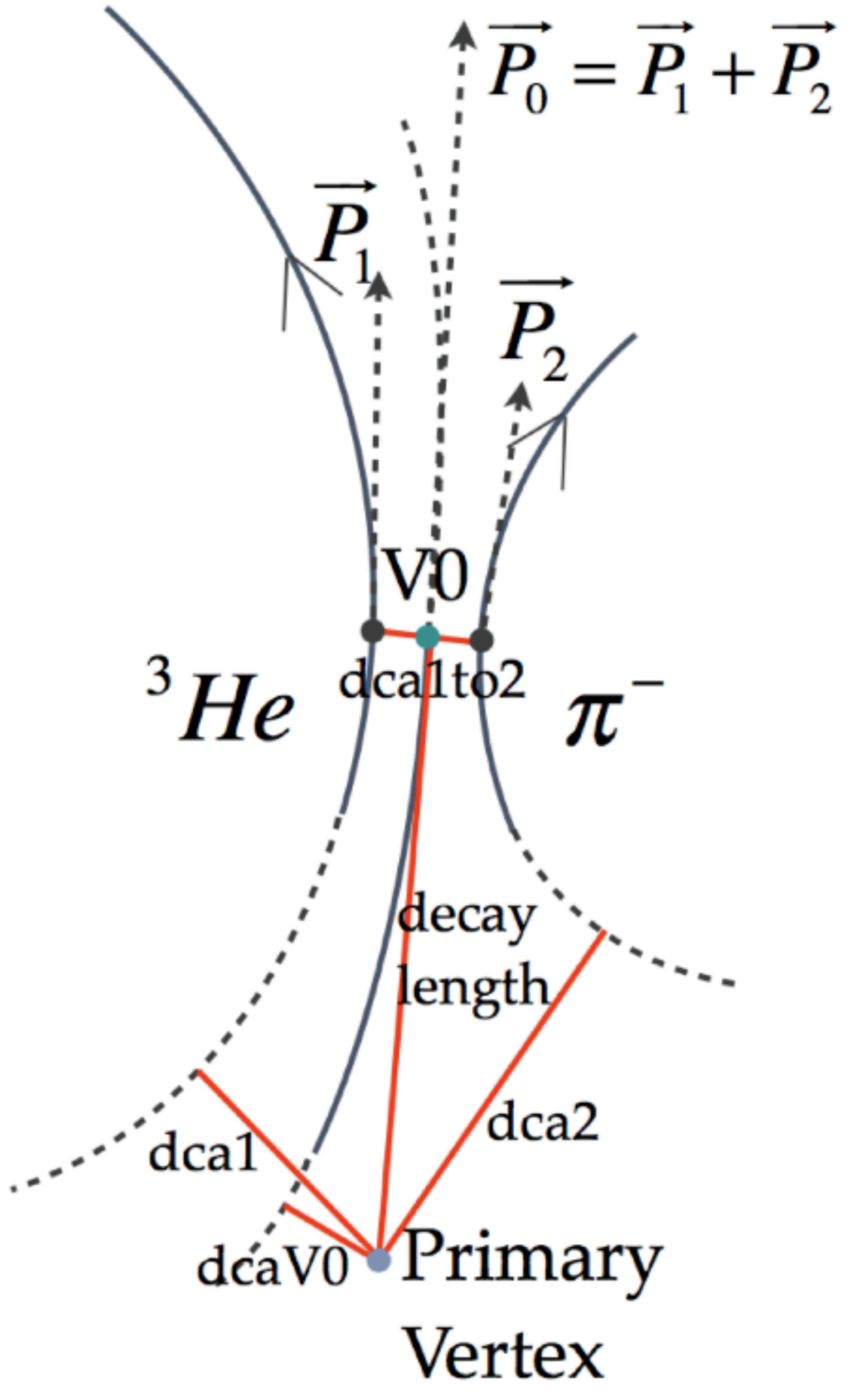

- Particle identification from energy loss measurement using TPC
- KF particle package[1] is used for signal reconstruction
- Hypernuclei reconstructed via their weak decay channels:

$^{3}_{\Lambda}\mathrm{H} \rightarrow {}^{3}\mathrm{He} + \pi^{-}$ $\quad$ $^{3}_{\Lambda}\mathrm{H} \rightarrow \mathrm{d} + \mathrm{p} + \pi^{-}$ $\quad$ $^{4}_{\Lambda}\mathrm{H} \rightarrow {}^{4}\mathrm{He} + \pi^{-}$ $\quad$ $^{4}_{\Lambda}\mathrm{He} \rightarrow {}^{3}\mathrm{He} + \mathrm{p} + \pi^{-}$

[1]Zyzak M, Kisel I, Senger P. Online selection of short-lived particles on many-core computer architectures in the CBM experiment at FAIR[R]. Collaboration FAIR: CBM, 2016.

Hypernuclei signal reconstruction

2-body decay channels: STAR, PRL 128, 202301(2022)

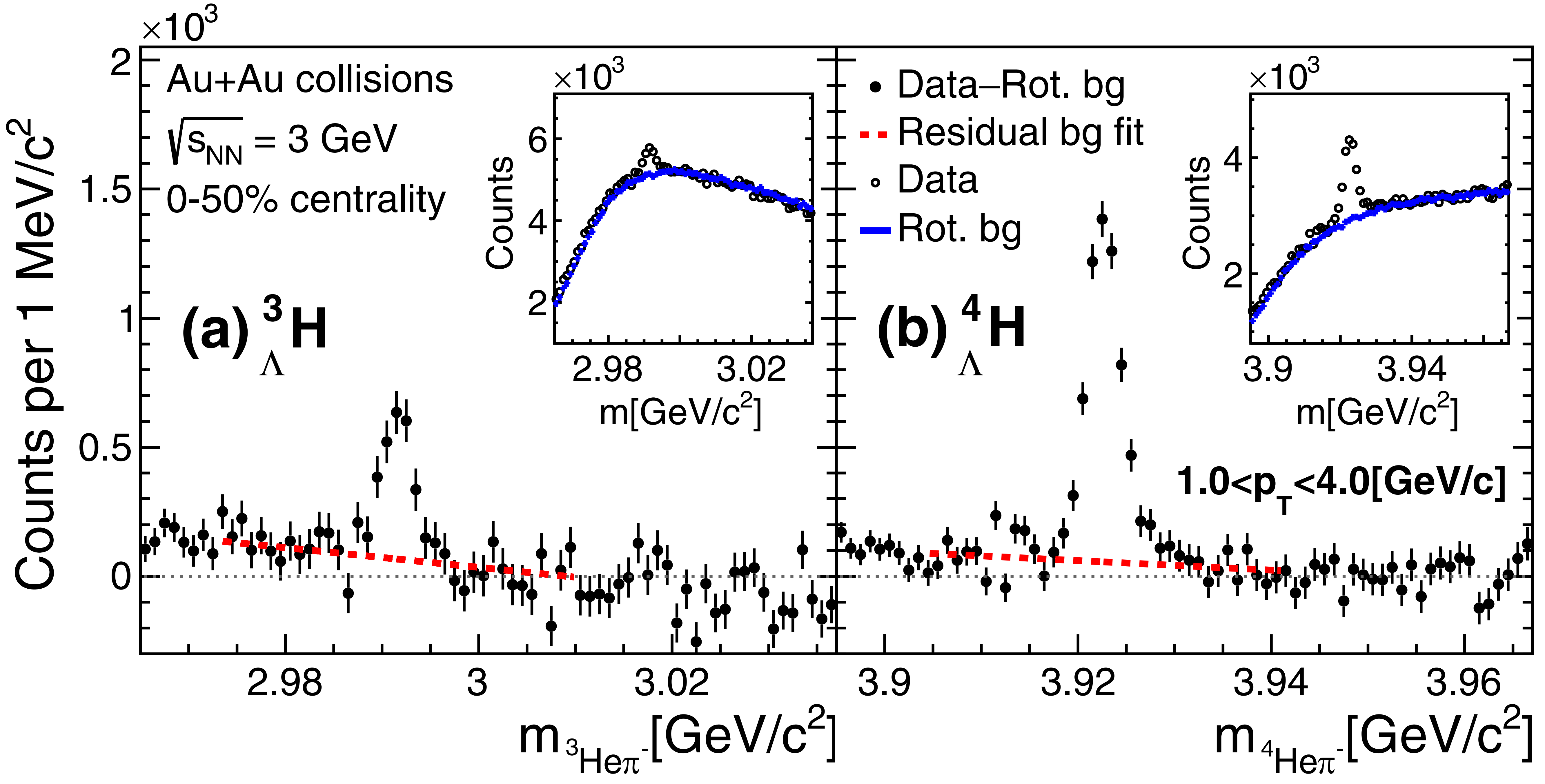

3-body decay channels: Xiujun Li@ATHIC2023

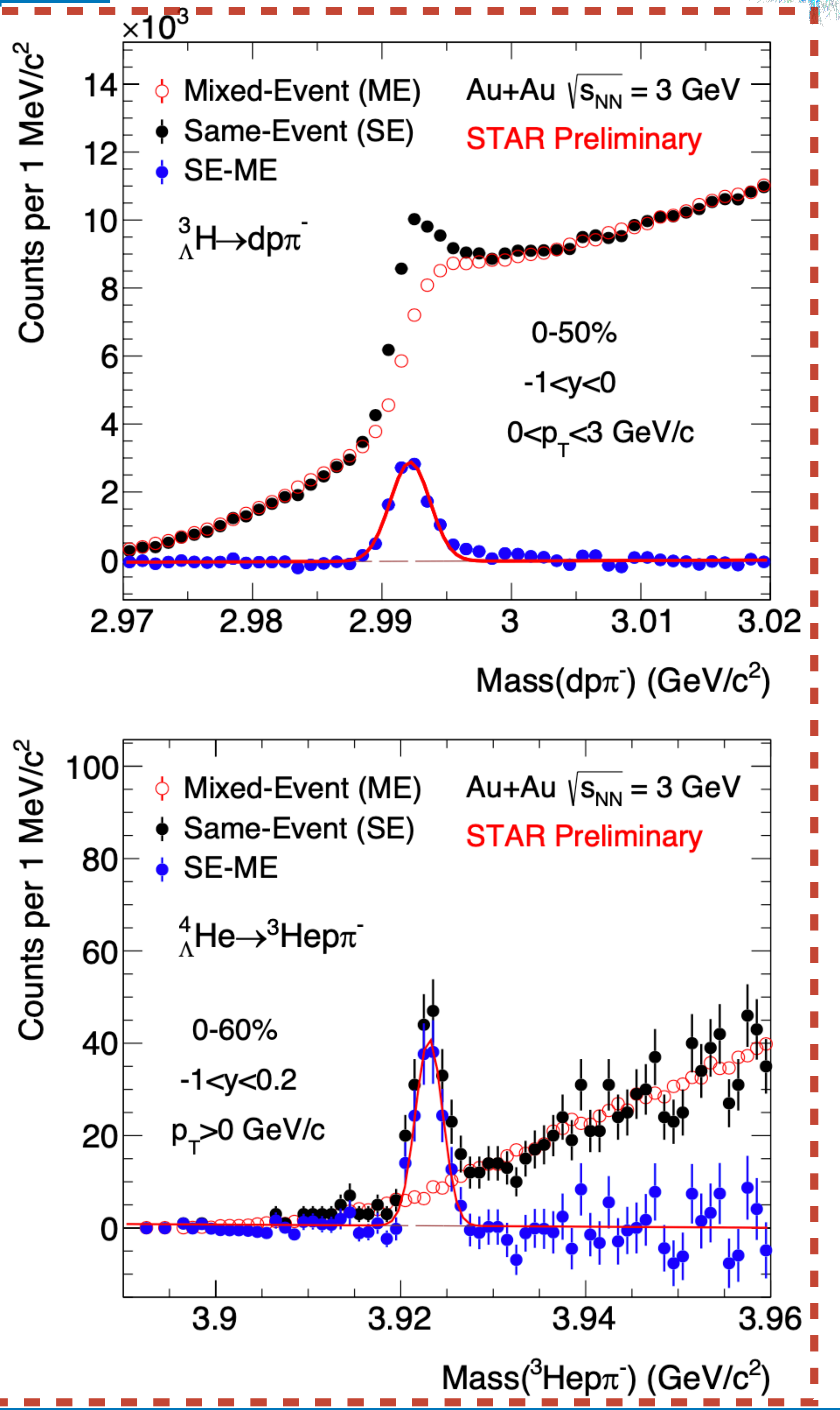

- Combinatorial background estimated via:
  - Rotating daughter tracks
  - Event mixing

${}^{3}_{\Lambda}$H branching ratio R_3

Relative branching ratio: $R_3 = \dfrac{B.R.({}^{3}_{\Lambda}H \rightarrow {}^{3}He\pi^-)}{B.R.({}^{3}_{\Lambda}H \rightarrow {}^{3}He\pi^-) + B.R.({}^{3}_{\Lambda}H \rightarrow dp\pi^-)}$

F. Hildenbrand et al. PRC 102, 064002 (2020)

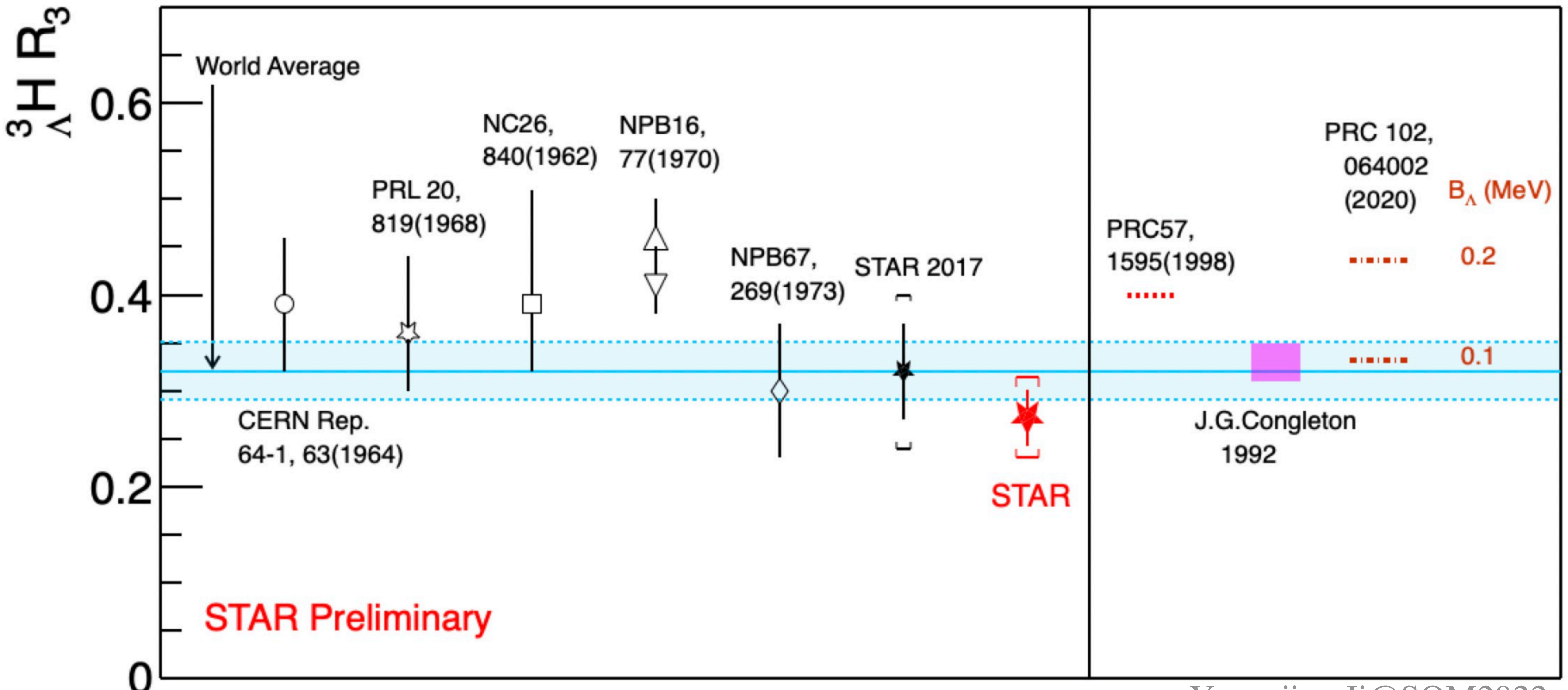

Yuangjing Ji@SQM2022

- Recent calculation shows that R_3 may be sensitive to the binding energy (B_Λ) of ${}^{3}_{\Lambda}$H
  - $B_\Lambda \rightarrow$ provide constraints to Y-N interaction

- Using $\sqrt{s_{NN}}$ = 3.0 GeV data:
  - $R_3 = 0.272 \pm 0.030(stat.) \pm 0.042(syst.)$
  - Model comparison suggesting a weakly-bounded state for ${}^{3}_{\Lambda}$H

- Improved precision on R_3
  - Stronger constraints on absolute B.R.s and ${}^{3}_{\Lambda}$H internal structure models

${}^{3}_{\Lambda}$H, ${}^{4}_{\Lambda}$H and ${}^{4}_{\Lambda}$He lifetimes

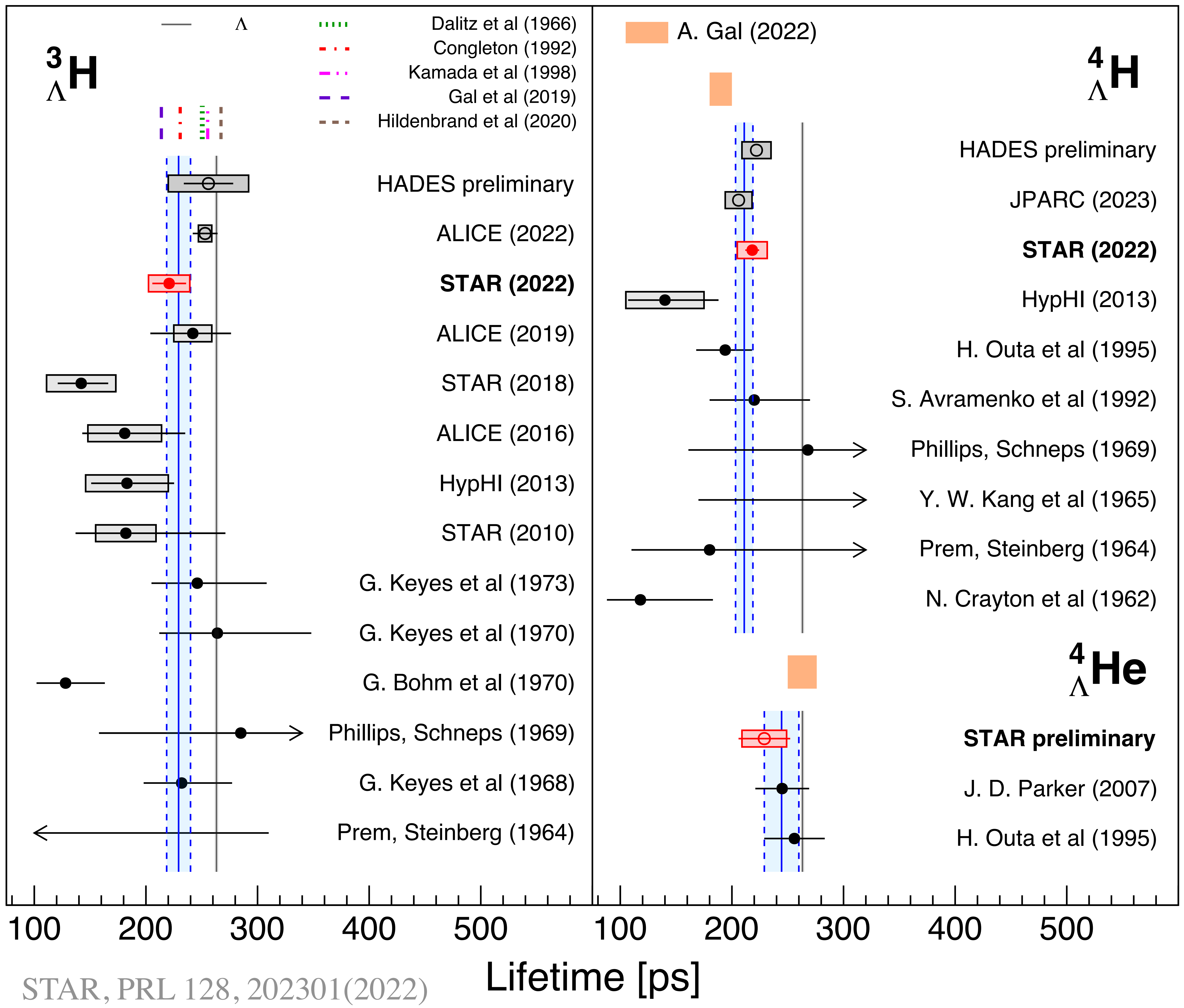

STAR, PRL 128, 202301(2022)
${}^{3}_{\Lambda}$H: ALICE(2022),arXiv:2209.07360
${}^{4}_{\Lambda}$H: JPARC(2023),arXiv:2302.07443

Xiujun Li@ATHIC2023

Using $\sqrt{s_{NN}}$ = 3.0 GeV and 7.2 GeV datasets:

${}^{3}_{\Lambda}$H: $\tau = 221 \pm 15(\text{stat.}) \pm 19(\text{syst.})[\text{ps}]$

${}^{4}_{\Lambda}$H: $\tau = 218 \pm 6(\text{stat.}) \pm 13(\text{syst.})[\text{ps}]$

${}^{4}_{\Lambda}$He: $\tau = 229 \pm 23(\text{stat.}) \pm 20(\text{syst.})[\text{ps}]$

- Indication of shorter lifetimes for ${}^{3}_{\Lambda}$H, ${}^{4}_{\Lambda}$H and ${}^{4}_{\Lambda}$He than that of free Λ (with 1.8σ, 3.0σ, 1.1σ respectively)
- Consistent with former measurements and world average values
- $\tau_{{}^{3}_{\Lambda}H}$: consistent with calculation including pion FSI[1] and calculation with Λd 2-body picture[2] within 1σ
- $\tau_{{}^{4}_{\Lambda}H}$ and $\tau_{{}^{4}_{\Lambda}He}$: consistent with expectations from isospin rule

Precision ${}^{3}_{\Lambda}$H and ${}^{4}_{\Lambda}$H measurements provide tight constraints on models.

[1]A. Gal and H. Garcilazo, PLB 791, 48 (2019)
[2]J.G. Congleton, J. Phys. G 18, 339 (1992)

B_Λ and ΔB_Λ of ${}^4_\Lambda$H and ${}^4_\Lambda$He

STAR, PLB 834, 137449 (2022)

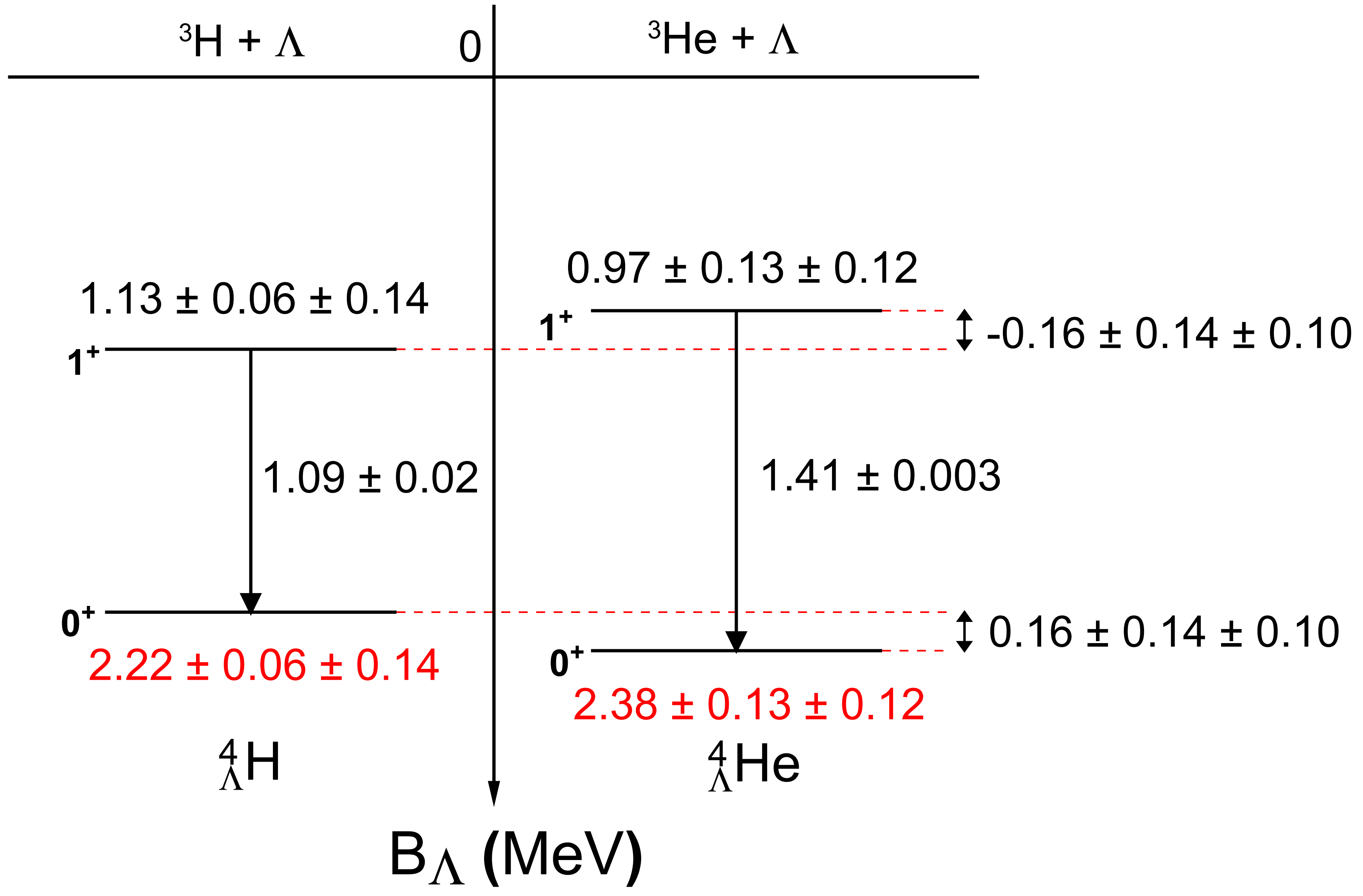

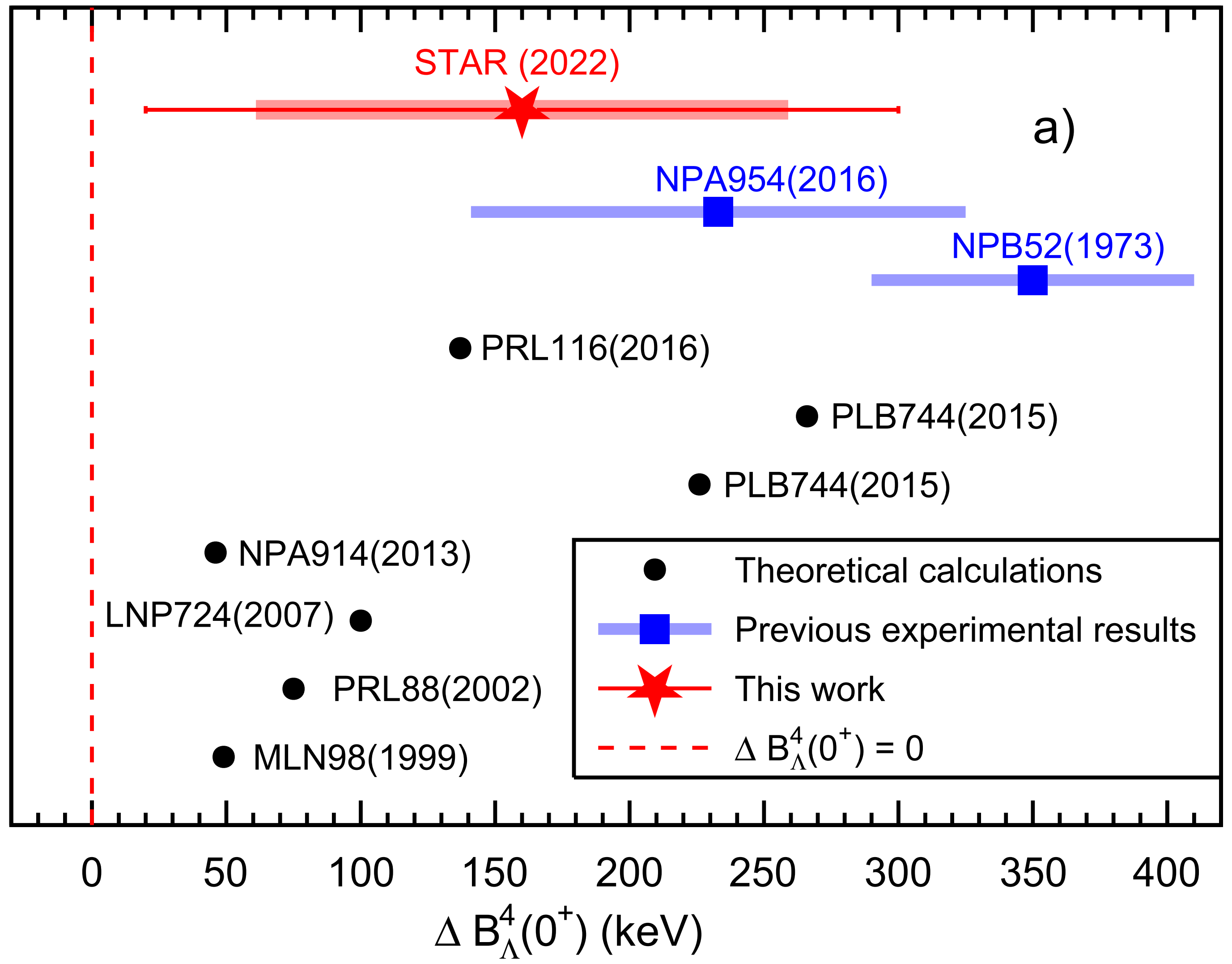

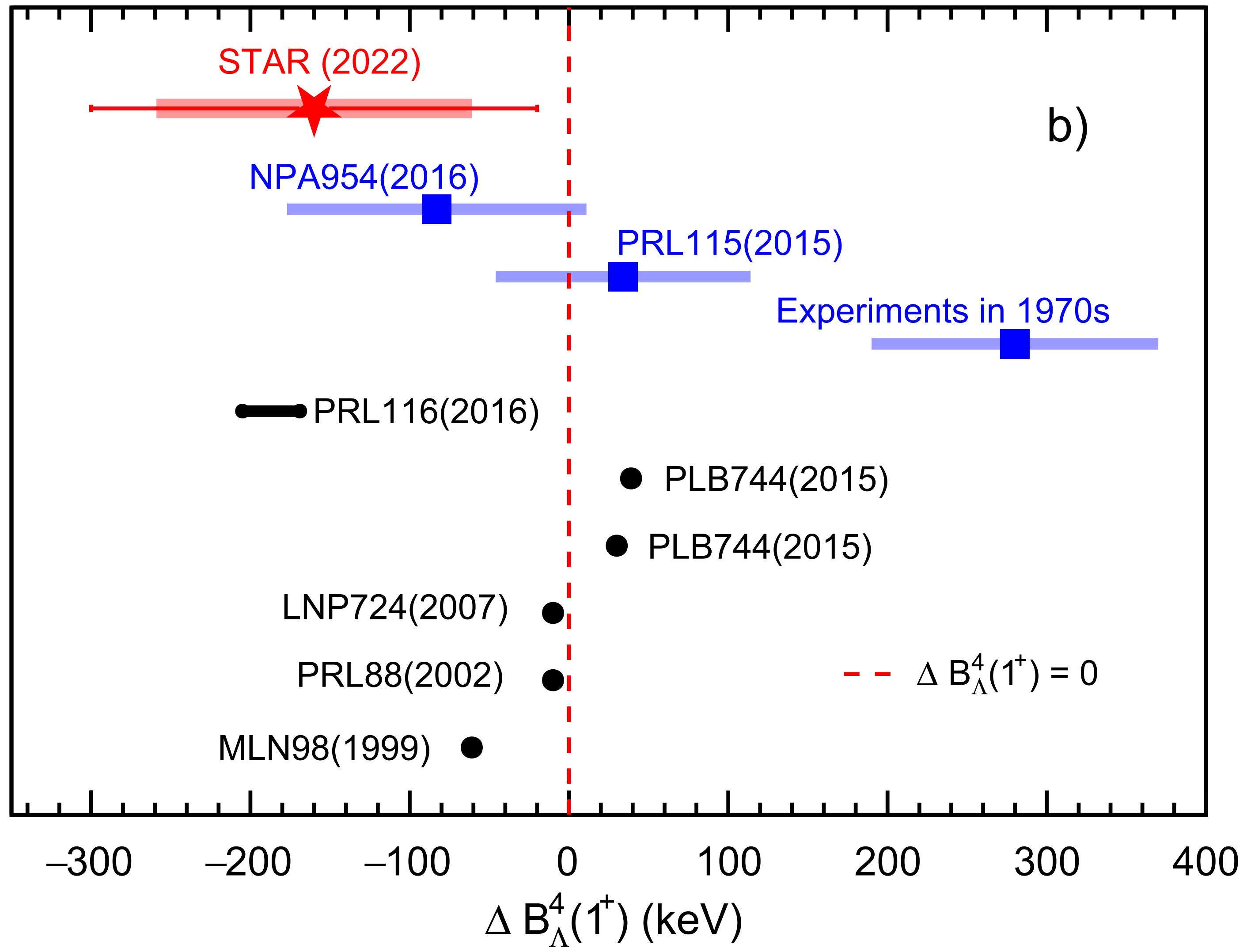

- Λ binding energy $B_\Lambda = (M_\Lambda + M_{\text{core}} - M_{\text{hypernucleus}})c^2$
  - The ground state B_Λ are directly measured:

    $$\Delta \mathrm{B}^4_\Lambda(0^+) = \mathrm{B}_\Lambda({}^4_\Lambda\mathrm{He},0^+) - \mathrm{B}_\Lambda({}^4_\Lambda\mathrm{H},0^+)$$

  - For excited states, the results are obtained by combining with the γ-ray transition energies E_γ J-PARC E13, PRL 115, 222501(2015) CERN-Lyon-Warsaw, PLB. 62, 467 (1976)

    $$\mathrm{B}^4_\Lambda({}^4_\Lambda\mathrm{He/H},1^+) = \mathrm{B}_\Lambda({}^4_\Lambda\mathrm{He/H},0^+) - \mathrm{E}_\gamma({}^4_\Lambda\mathrm{He/H})$$

    $$\Delta \mathrm{B}^4_\Lambda(1^+) = \mathrm{B}_\Lambda({}^4_\Lambda\mathrm{He},1^+) - \mathrm{B}_\Lambda({}^4_\Lambda\mathrm{H},1^+)$$

- Mirror hypernuclei ${}^4_\Lambda$H and ${}^4_\Lambda$He: opportunity to study charge symmetry breaking (CSB) effect in A = 4 hypernuclei
  - CSB in 0^+ and 1^+ states are comparable and have opposite signs
    - Consistent with theoretical calculations within large uncertainties

Hypernuclei production at 3 GeV

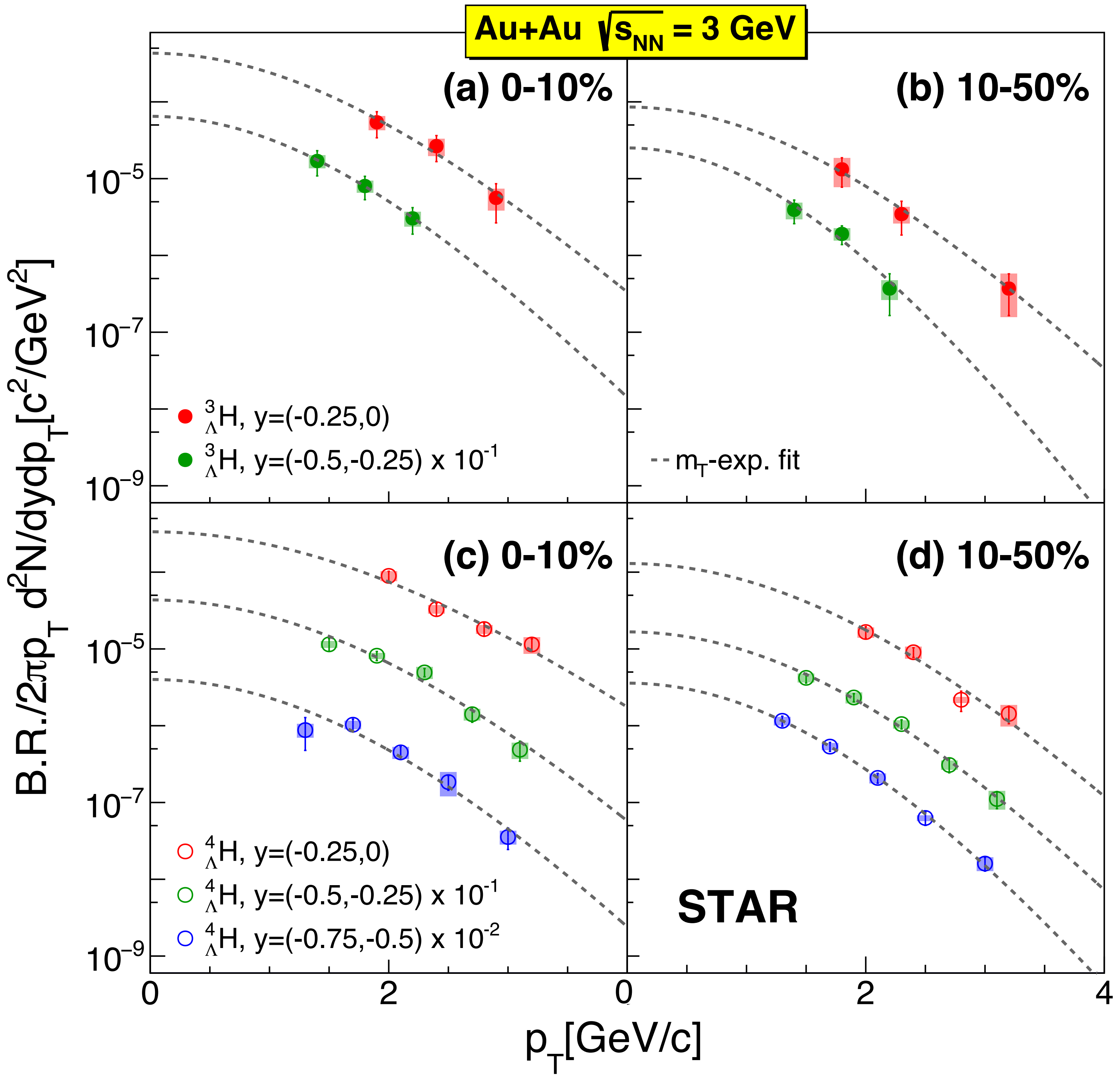

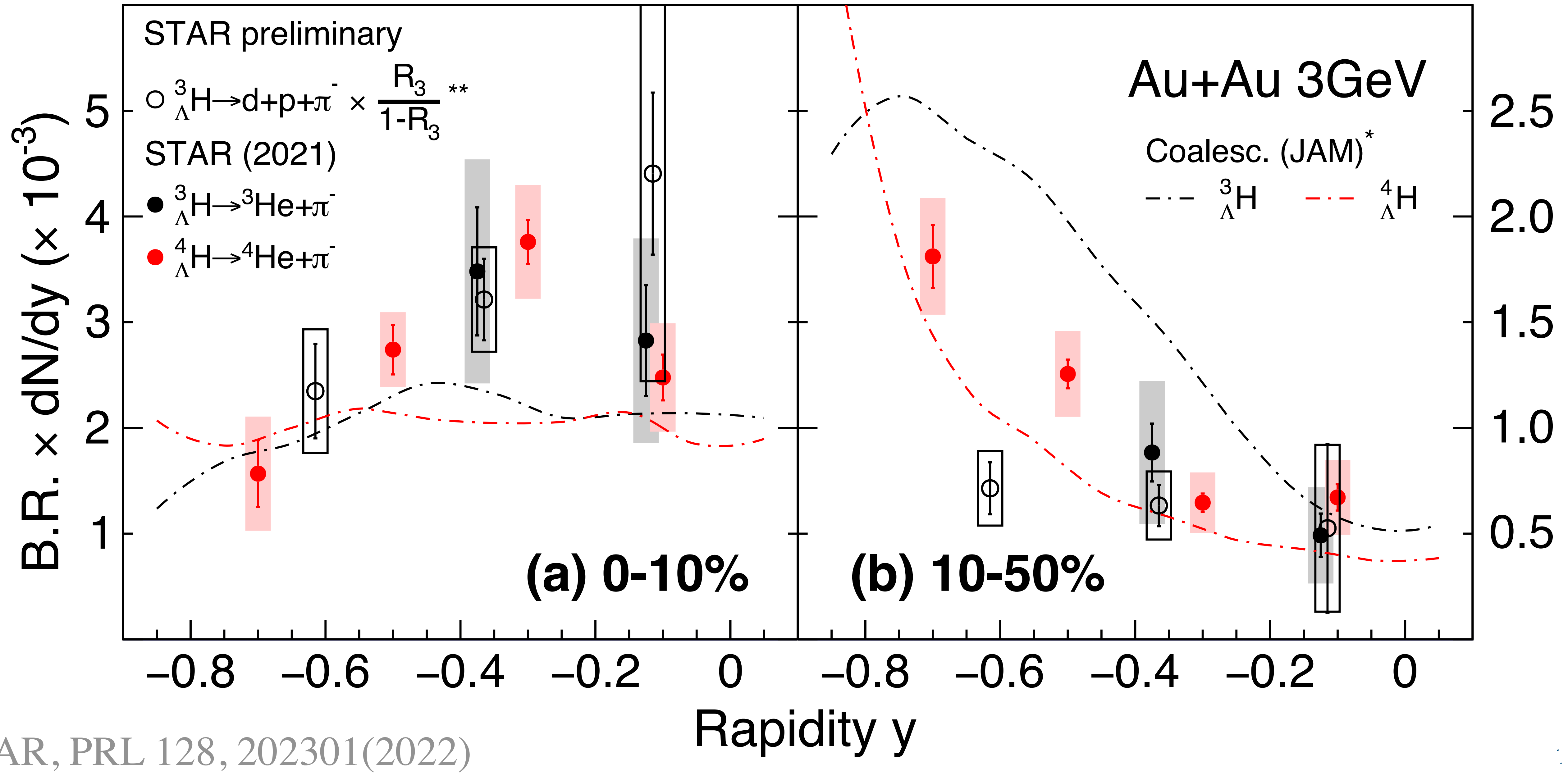

STAR, PRL 128, 202301(2022)

Xiujun Li@ATHIC2023

- First measurement of dN/dy vs y for hypernuclei in heavy-ion collisions
- Different trends in the ${}^{4}_{\Lambda}\mathrm{H}$ rapidity distribution in central (0-10%) and mid-central (10-50%) collisions at $\sqrt{s_{NN}}$ = 3.0 GeV

- Transport model (JAM) with coalescence approximately reproduces trends of ${}^{4}_{\Lambda}\mathrm{H}$ rapidity distributions seen in data, but fails to reproduce the trend of ${}^{3}_{\Lambda}\mathrm{H}$ in 10-50%

$^{3}_{\Lambda}$H and $^{4}_{\Lambda}$H directed flow at 3 GeV

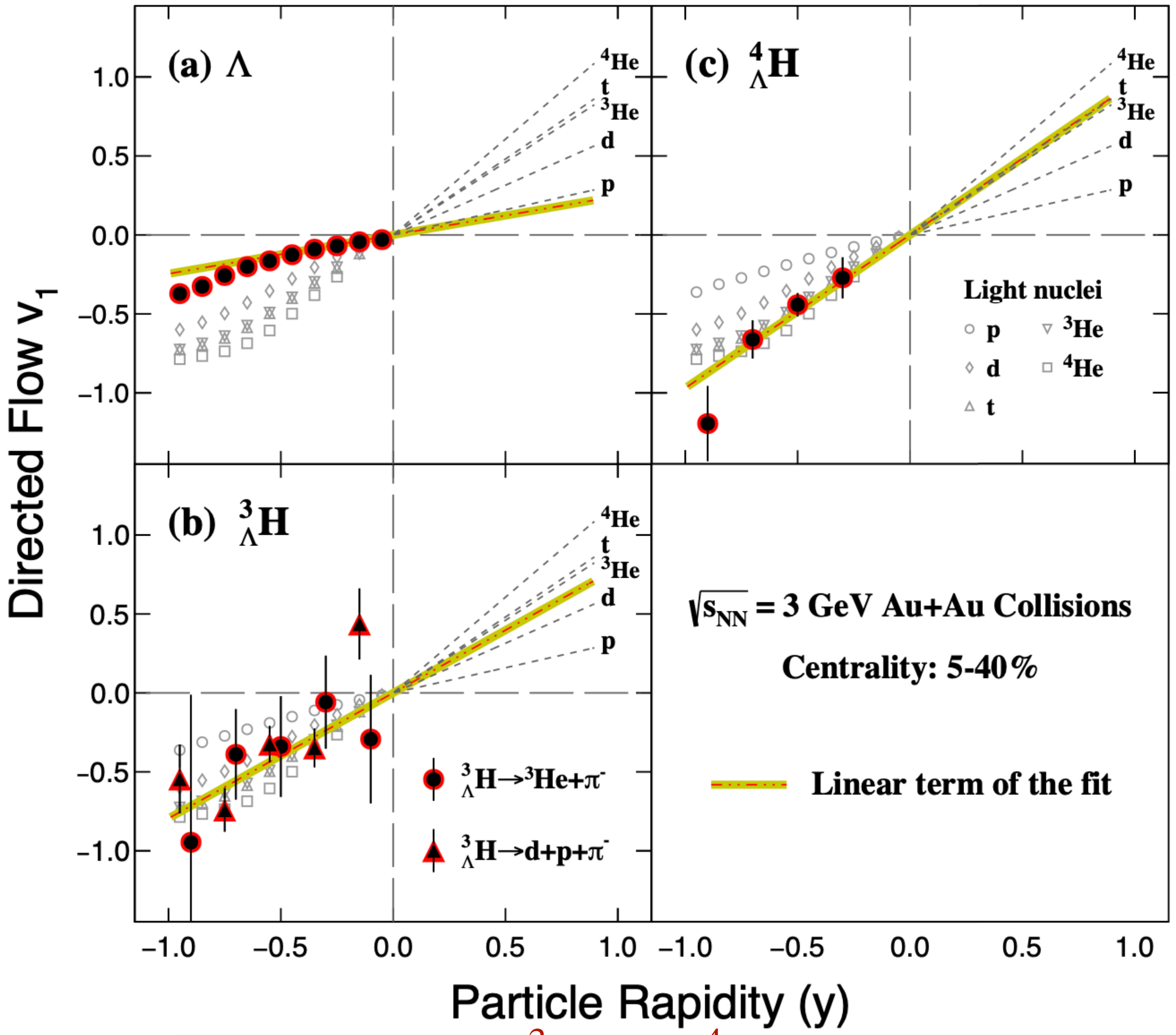

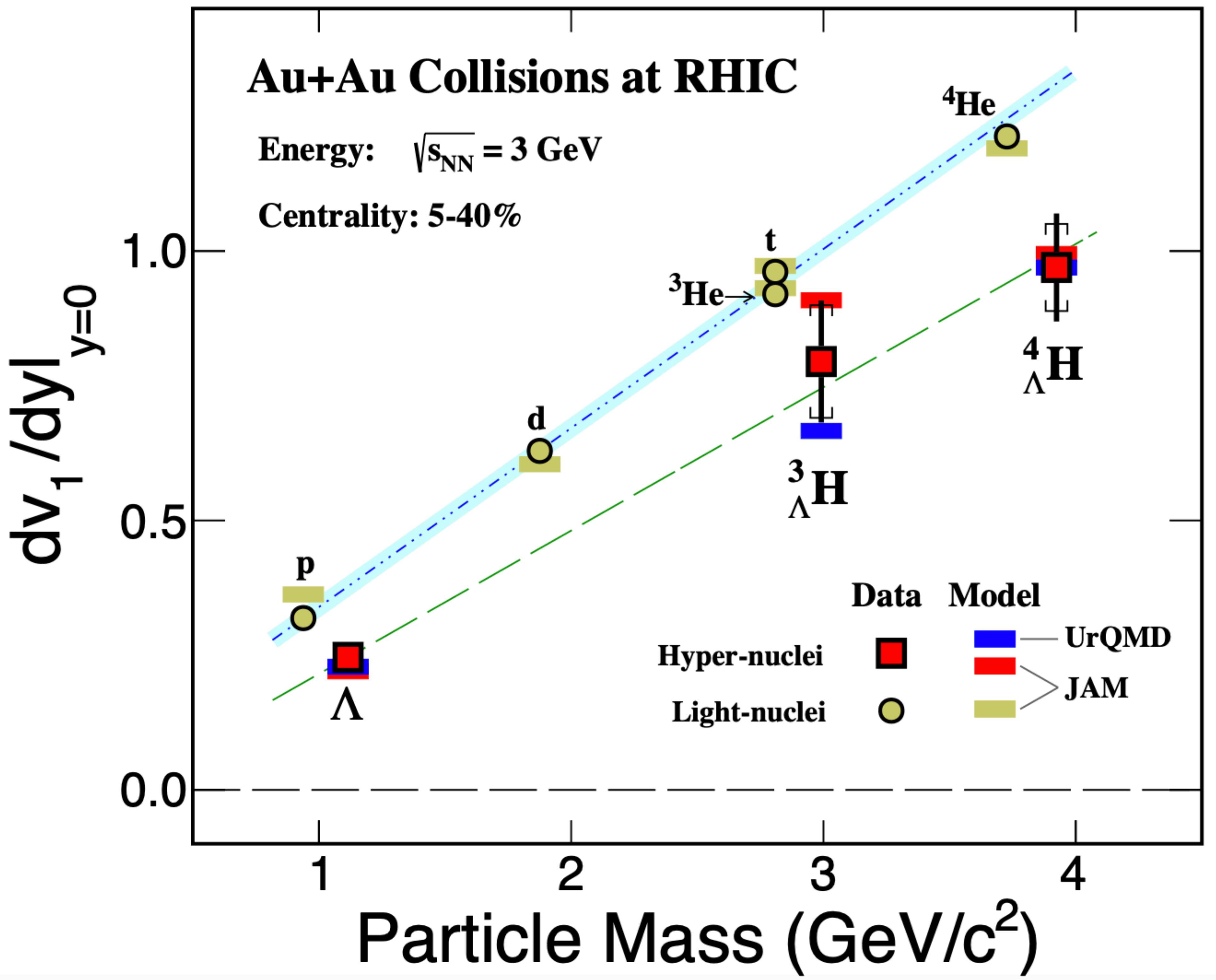

arXiv:2211.16981
accepted by PRL

- First observation of $^{3}_{\Lambda}$H and $^{4}_{\Lambda}$H directed flow (v_1) in mid-central 5-40% Au+Au collisions at 3 GeV
- Mid-rapidity v_1 slopes of $^{3}_{\Lambda}$H and $^{4}_{\Lambda}$H follow baryon mass scaling.

→ Imply coalescence process to be the dominant formation mechanism for $^{3}_{\Lambda}$H and $^{4}_{\Lambda}$H production in 3 GeV Au+Au collisions

Energy dependence of hypernuclei production in heavy-ion collisions

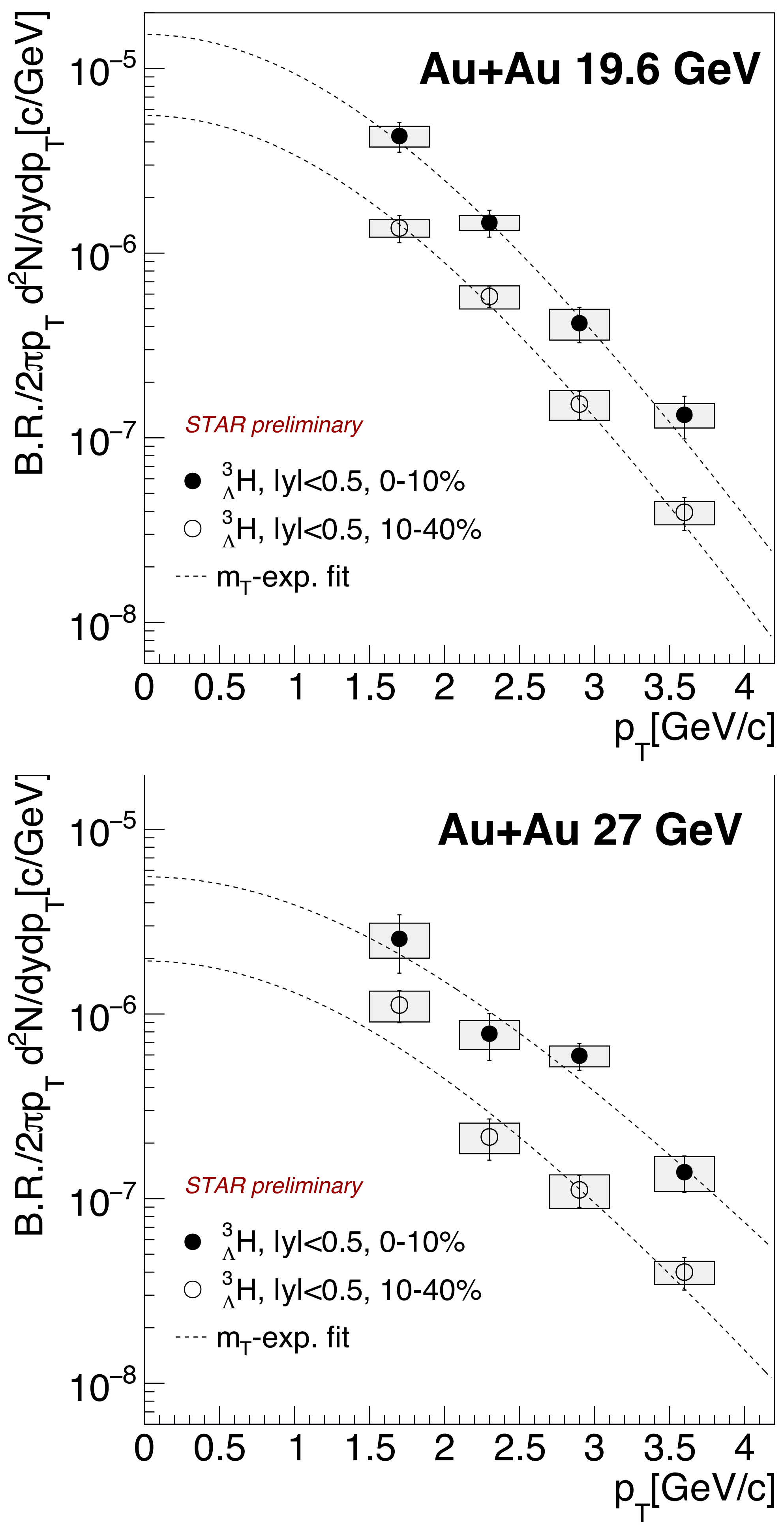

- $^{3}_{\Lambda}$H mid-rapidity yields obtained as a function of p_T and centrality at 19.6 and 27 GeV

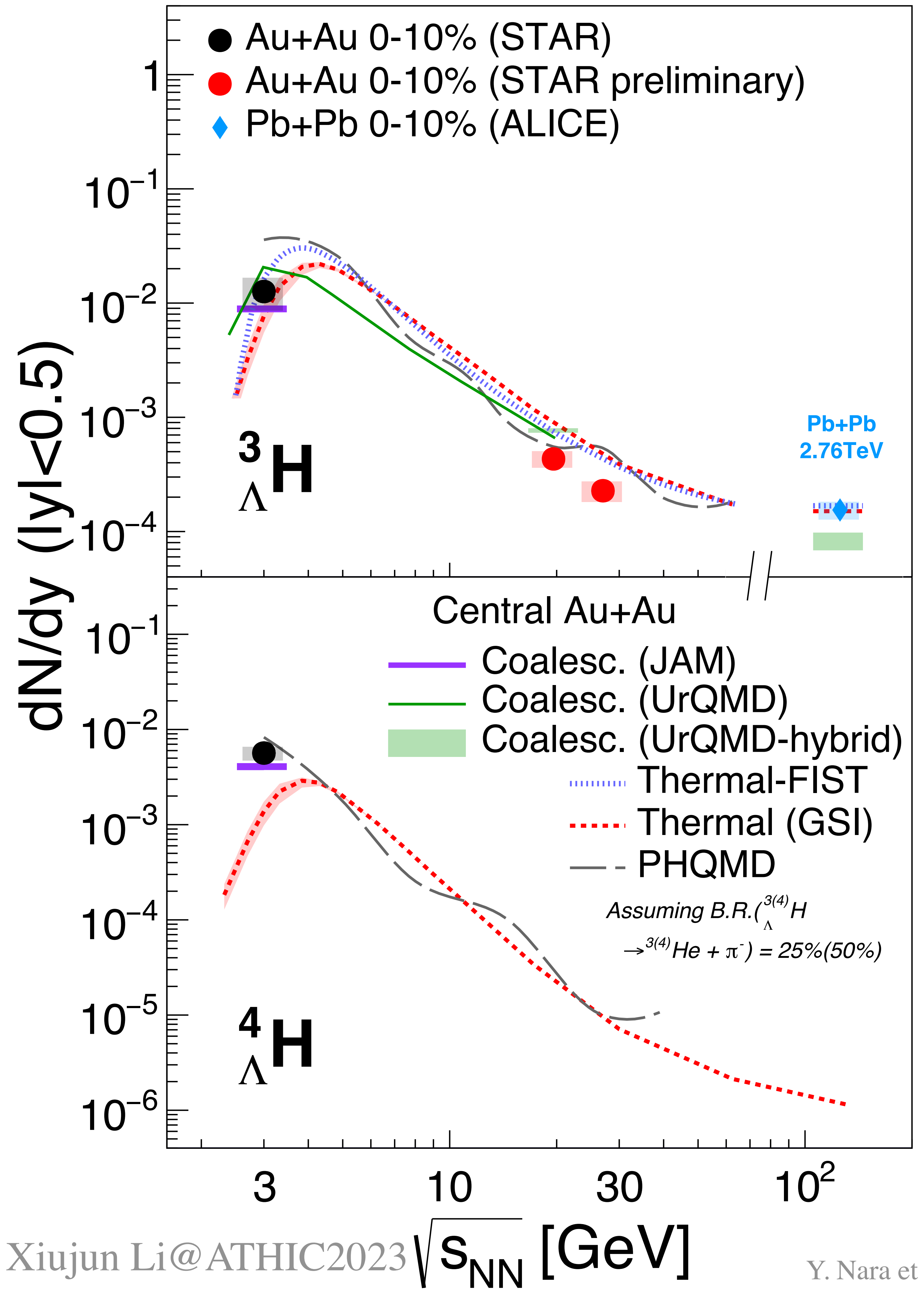

Xiujun Li@ATHIC2023

STAR, PRL 128 (2022) 202301
ALICE, PLB 754 (2016) 360

- $^{3}_{\Lambda}$H yield at mid-rapidity increases from 2.76 TeV to 3 GeV
  - Driven by increase in baryon density at low energies
- Thermal(GSI), Coalescence(UrQMD), Thermal-FIST and PHQMD reproduce the trend

For Au+Au @ 3 GeV

- Coalescence(JAM) with tuned parameters can describe data
- PHQMD describes $^{4}_{\Lambda}$H, but overestimates $^{3}_{\Lambda}$H

First energy dependence of hypernuclei production yields in the high-baryon-density region

- Provide **first constraints** for hypernuclei production models in the high-baryon-density region

Y. Nara et al, PRC 61 (1999) 024901 (JAM)
S. Gläßel et al, arXiv: 2106,14839 (PHQMD)
A. Andronic et al, PLB 697 (2011) 203 (Thermal (GSI))
T. Reichert, J. Steinheimer et al, arXiv:2210.11876(2022) (UrQMD, Thermal-FIST)

Hyper-to-light nuclei comparison at 3 GeV

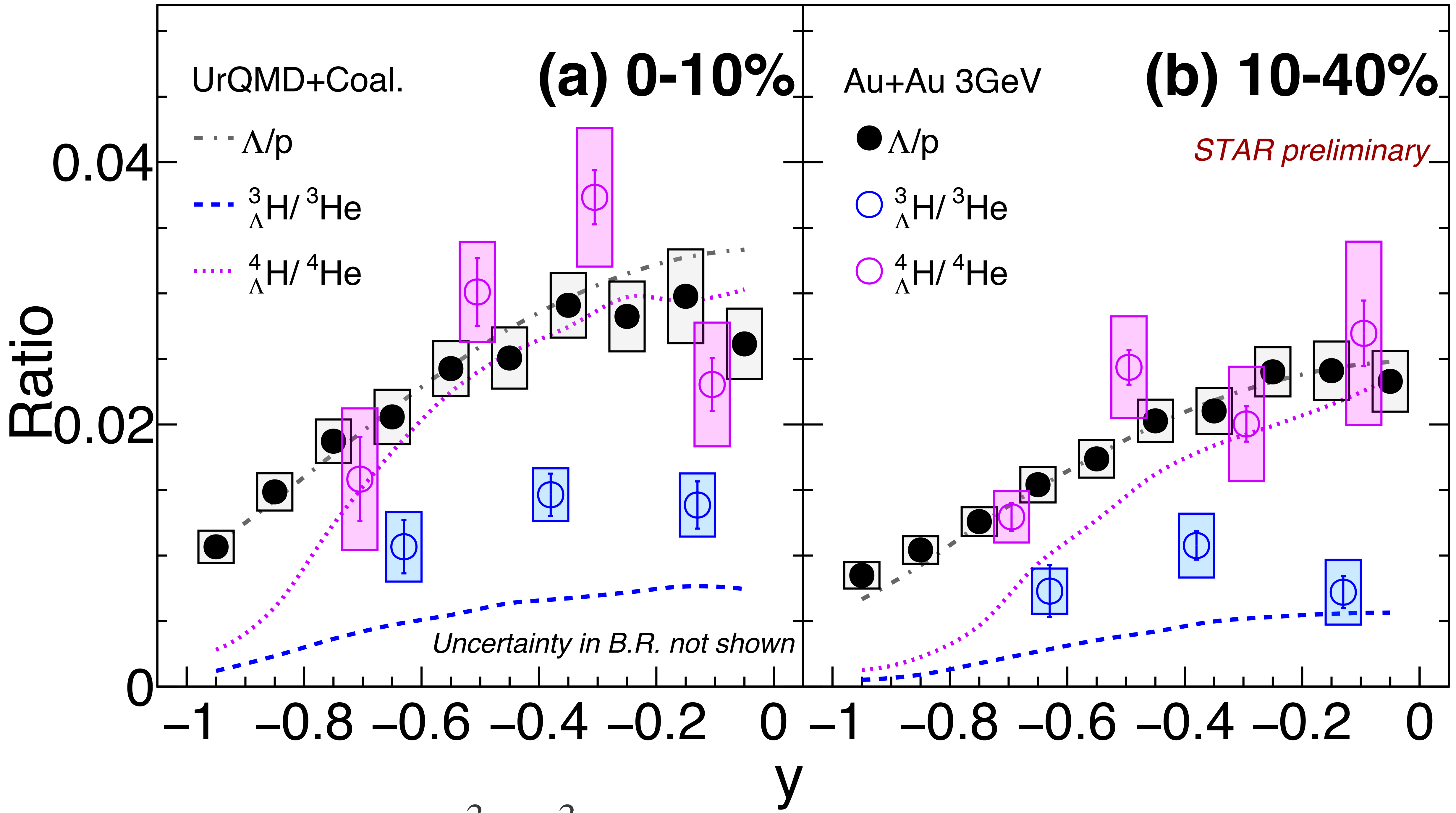

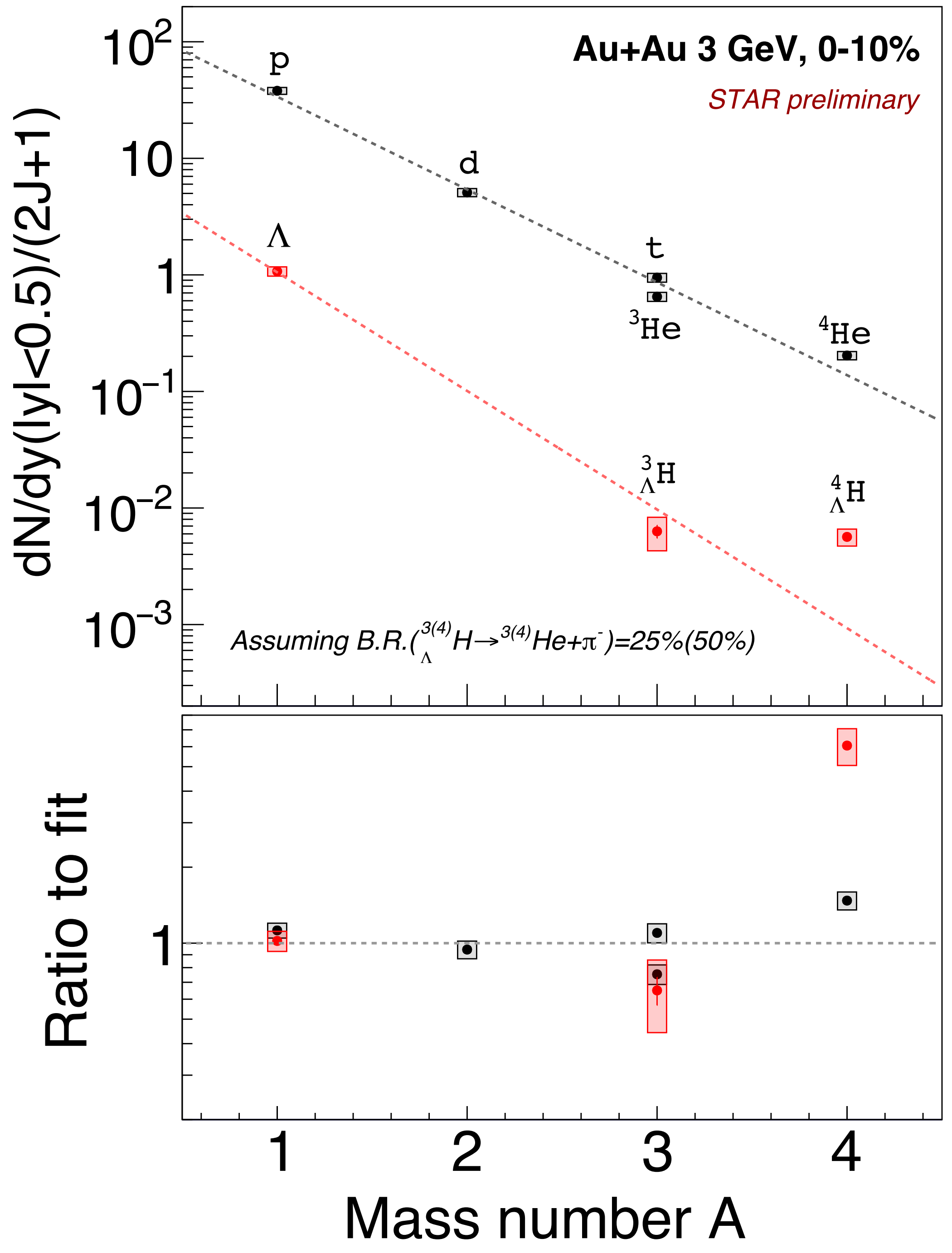

A. Andronic et al, PLB 697 (2011) 203 (Thermal model)

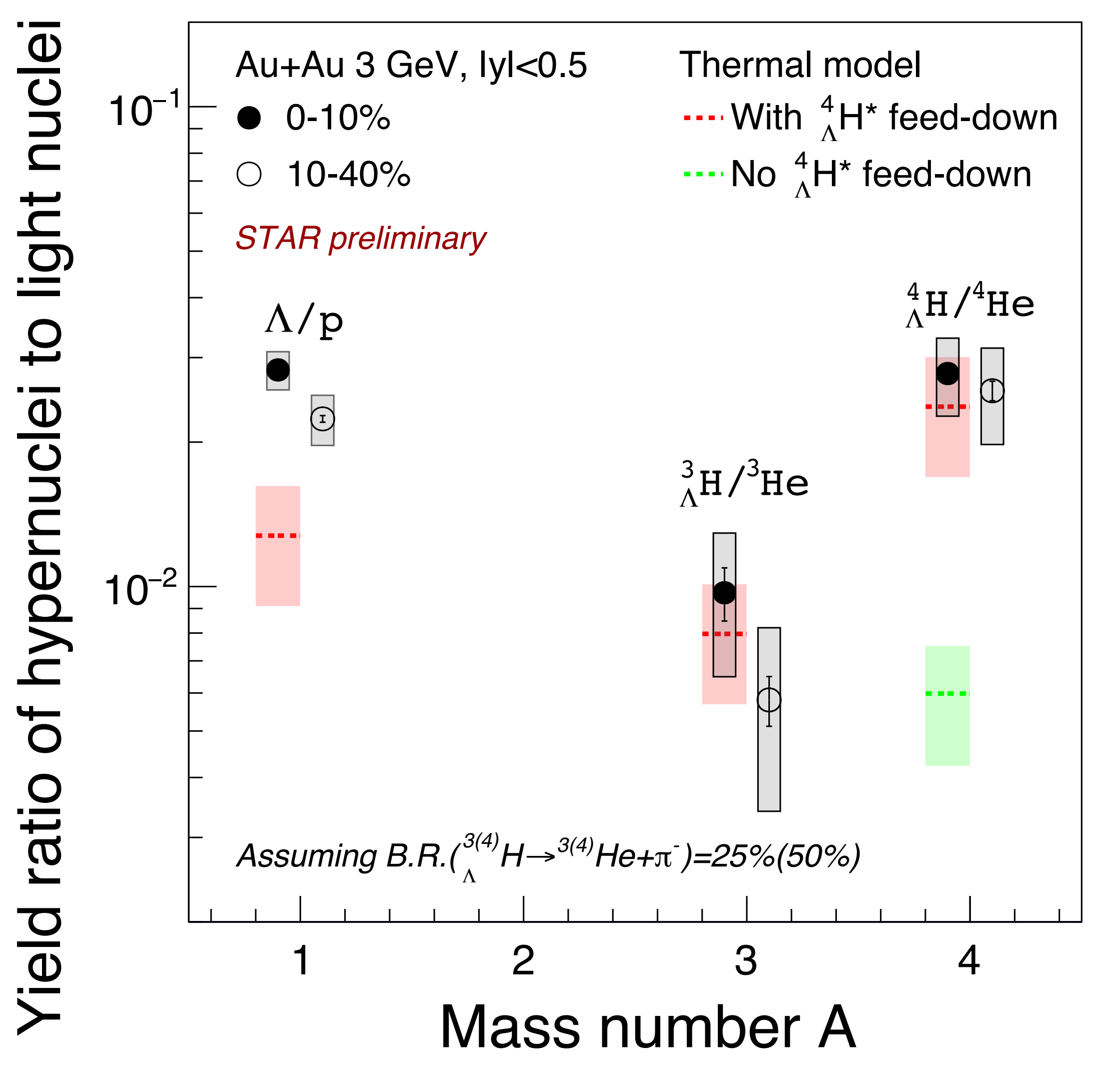

Xiujun Li@ATHIC2023

- **Suppression of $^{3}_{\Lambda}\mathrm{H}/^{3}\mathrm{He}$ yield ratios compared to that of Λ/p**
  - Observed at both 0-10% and 10-40% centrality in Au+Au collisions at 3 GeV.
- **The $^{4}_{\Lambda}\mathrm{H}/^{4}\mathrm{He}$ yield ratios are comparable to that of Λ/p**
- **UrQMD model with coalescence describes the tendency of the distributions reasonably well, suggesting coalescence mechanism for hypernuclei formation.**

- **Non-monotonic behavior in light-to-hyper-nuclei ratio vs A**
- **Thermal model calculations including excited $^{4}_{\Lambda}\mathrm{H}^{*}$ feed-down show a similar trend**
  - Feed-down from excited state enhances $^{4}_{\Lambda}\mathrm{H}$ production

Suggest coalescence mechanism and creation of excited A = 4 hypernuclei

$S_{3,4}$ at 3 GeV

- Strangeness population factor S_A
  - Relative suppression of hypernuclei production compared to light nuclei production

$$S_A = \frac{{}^{A}_{\Lambda}H}{{}^{A}He \times \frac{\Lambda}{p}} = \frac{B_A({}^{A}_{\Lambda}H)(p_T)}{B_A({}^{A}He)(p_T)}$$

S.Zhang, PLB 684(2010)224

- B_A: Coalescence parameters

  - Expect ~1 if no suppression

$S_3 < 1$: relative suppression of ${}^{3}_{\Lambda}H/{}^{3}He$ compared to Λ/p

$S_4 \sim 1$, $S_4 > S_3$: ${}^{4}_{\Lambda}H/{}^{4}He$ is comparable to Λ/p

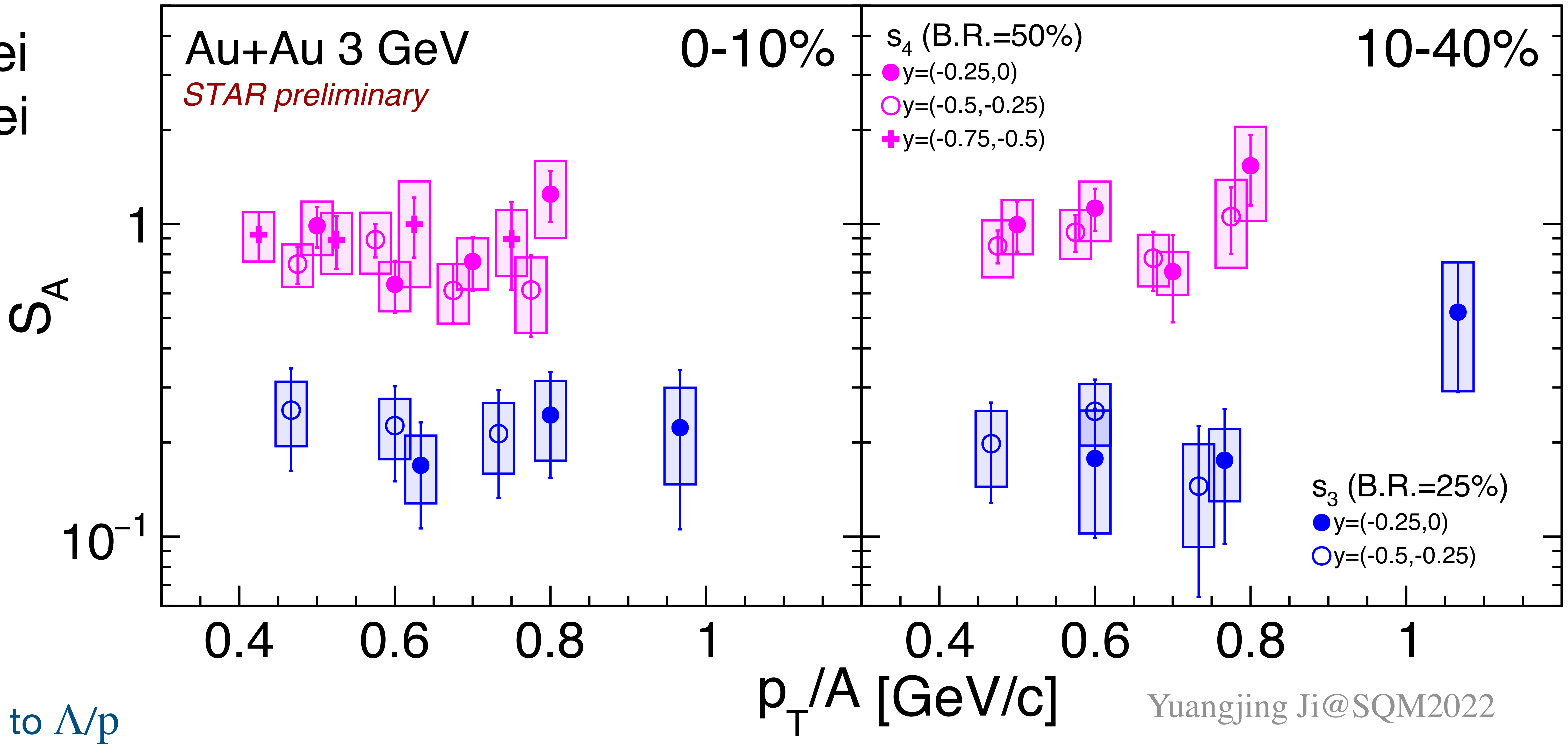

Yuangjing Ji@SQM2022

No obvious kinematic and centrality dependence of $S_{3,4}$ observed at 3 GeV.

→ Coalescence parameters B_A of ${}^{A}_{\Lambda}H$ and ${}^{A}He$ follow similar tendency versus p_T, rapidity and centrality, indicating that N-N and Y-N interactions that drive coalescence dynamics in these collisions are similar

Energy dependence of S_3

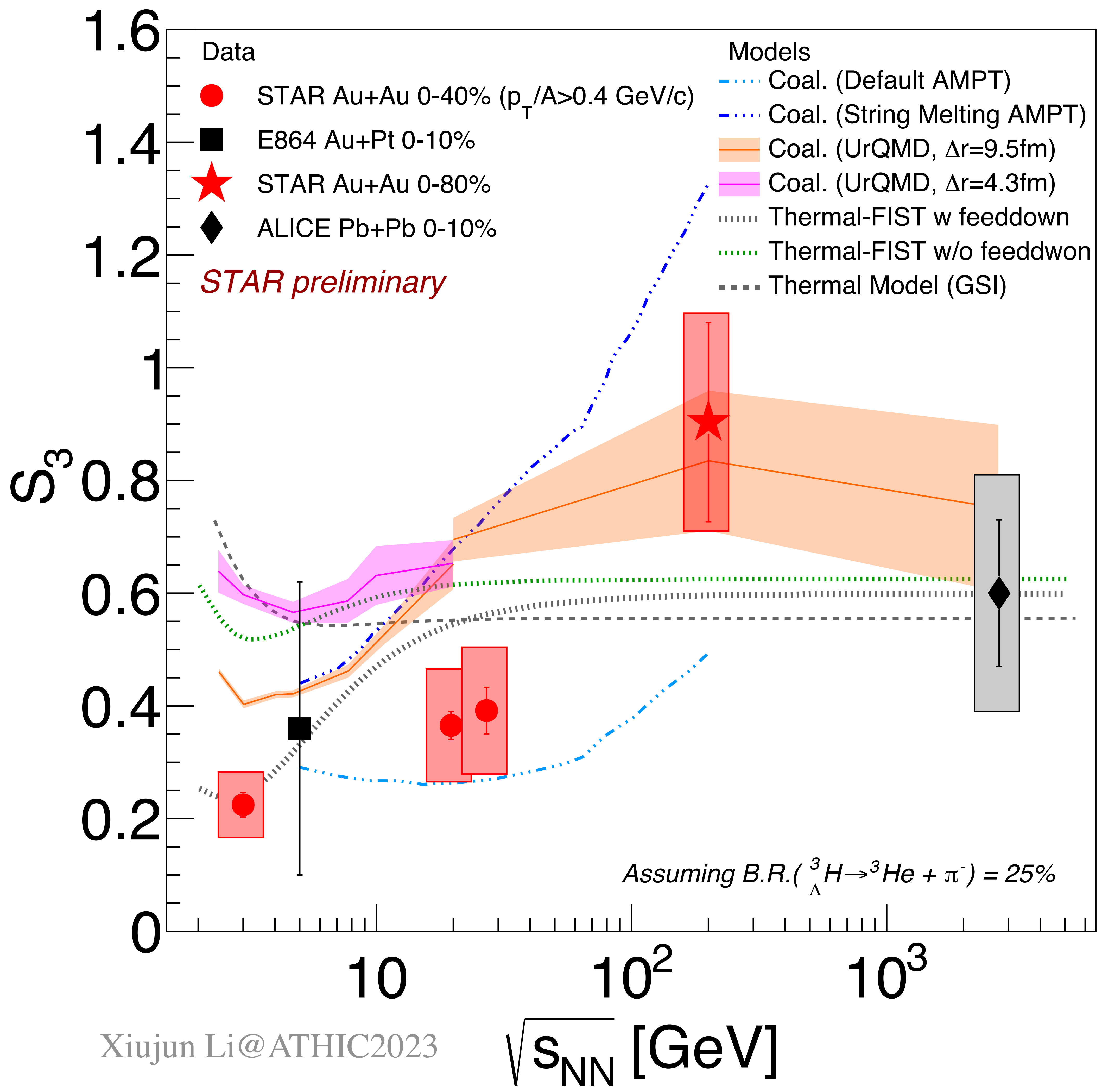

Xiujun Li@ATHIC2023

STAR, Science 328 (2010) 58
ALICE, PLB 754 (2016) 360
E864, PRC 70 (2004) 024902
NA49, J.Phys.Conf.Ser.110(2008)032010

A. Andronic et al, PLB 697 (2011) 203 (Thermal (GSI))
S. Zhang, PLB 684(2010)224 (Coal.+AMPT)
T. Reichert, J. Steinheimer et al, arXiv:2210.11876(2022) (UrQMD, Thermal-FIST)

- Data show a hint of an increasing trend from $\sqrt{s_{NN}}$ = 3.0 GeV to 2.76 TeV
- For coalescence models, the energy dependence is sensitive to the source radius (Δr)
- Thermal-FIST, which includes feed-down to p and ^{3}He from unstable nuclei, describes the S_3 data reasonably well

Provide constraints for hypernuclei production models in the high-baryon-density region

First observation of $^{4}_{\overline{\Lambda}}\overline{\mathrm{H}}$

See Tan Lu's poster@QM2022

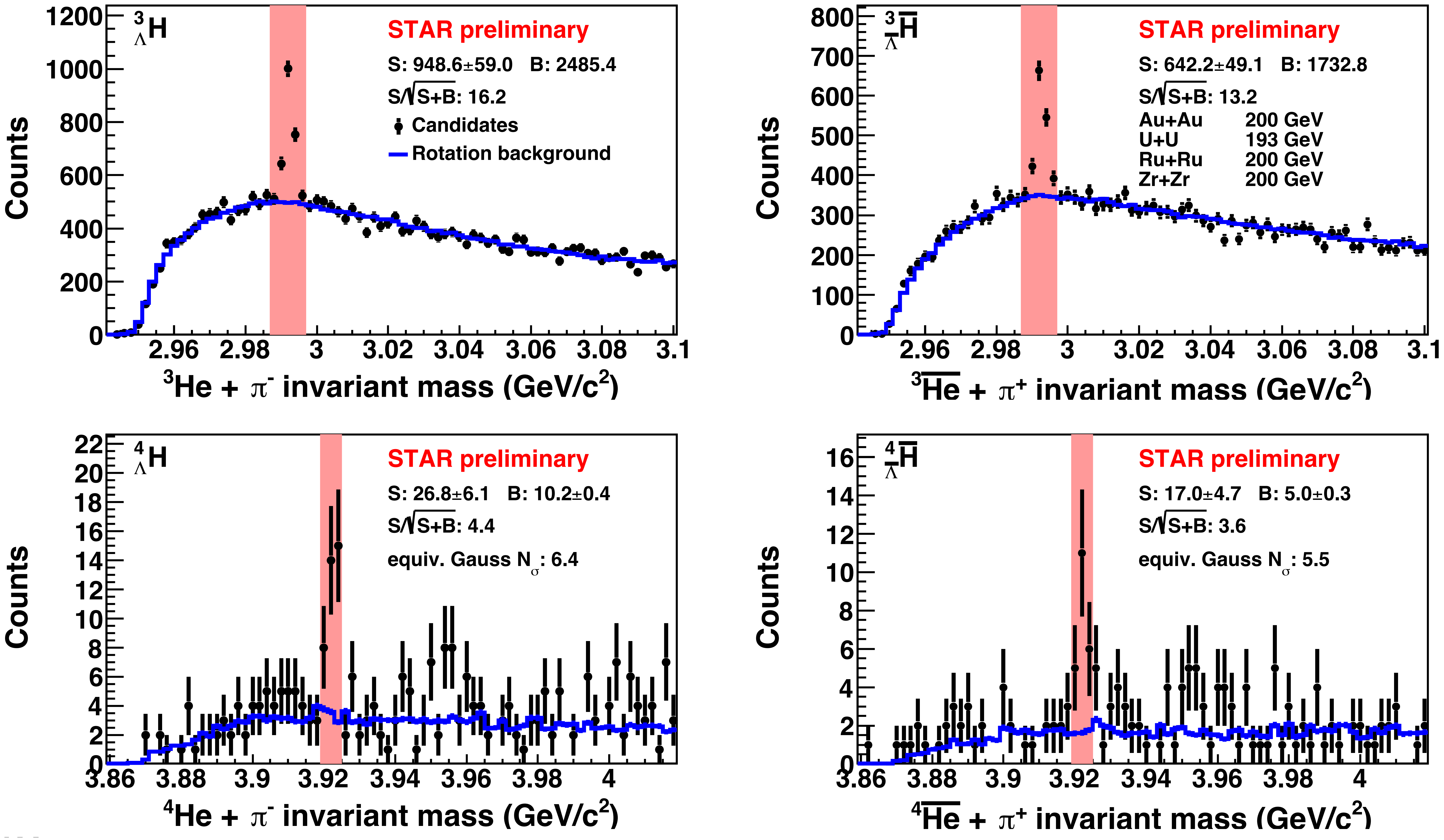

- The **heaviest antimatter hypernucleus** observed up to now
- New opportunity for the study of matter-antimatter asymmetry

- **First observation of $^{4}_{\overline{\Lambda}}\overline{\mathrm{H}}$ in experiment!**

Summary

Enhanced hypernuclei yields at low energies allow precision measurement.

- **Internal structure**
  - Precision ${}^{3}_{\Lambda}\mathrm{H}$, ${}^{4}_{\Lambda}\mathrm{H}$ lifetimes and relative branching ratio R_3 of ${}^{3}_{\Lambda}\mathrm{H}$ measured $\rightarrow$ strong constraints on hypernuclei models
  - Λ binding-energy difference between ${}^{4}_{\Lambda}\mathrm{H}$ and ${}^{4}_{\Lambda}\mathrm{He}$ shows hint of CSB effect for A=4 hypernuclei
- **Production**
  - v_1 slopes of Λ, ${}^{3}_{\Lambda}\mathrm{H}$ and ${}^{4}_{\Lambda}\mathrm{H}$ follow baryon mass scaling $\rightarrow$ support coalescence picture
  - First ${}^{3}_{\Lambda}\mathrm{H}$ and ${}^{4}_{\Lambda}\mathrm{H}$ dN/dy vs y and energy dependence of dN/dy @ high μ_{B} $\rightarrow$ constraints to hypernuclei production models
  - Relative suppression of ${}^{3}_{\Lambda}\mathrm{H}/{}^{3}\mathrm{He}$ compared to Λ/p and ${}^{4}_{\Lambda}\mathrm{H}/{}^{4}\mathrm{He}$ $\rightarrow$ support creation of ${}^{4}_{\Lambda}\mathrm{H}^{*}$, coalescence picture; weak centrality/kinematic dependence for S_3 and S_4
- **First discovery of ${}^{4}_{\Lambda}\overline{\mathrm{H}}$**

Outlook

1. iTPC and eToF fully installed in 2019 → extend η acceptance and improve PID at large η
2. High statistics data in STAR BES-II $\sqrt{s_{NN}}$ = 3.0 - 54.4 GeV, especially the **2 billion events** collected at 3 GeV in 2021 → larger statistics, higher precision

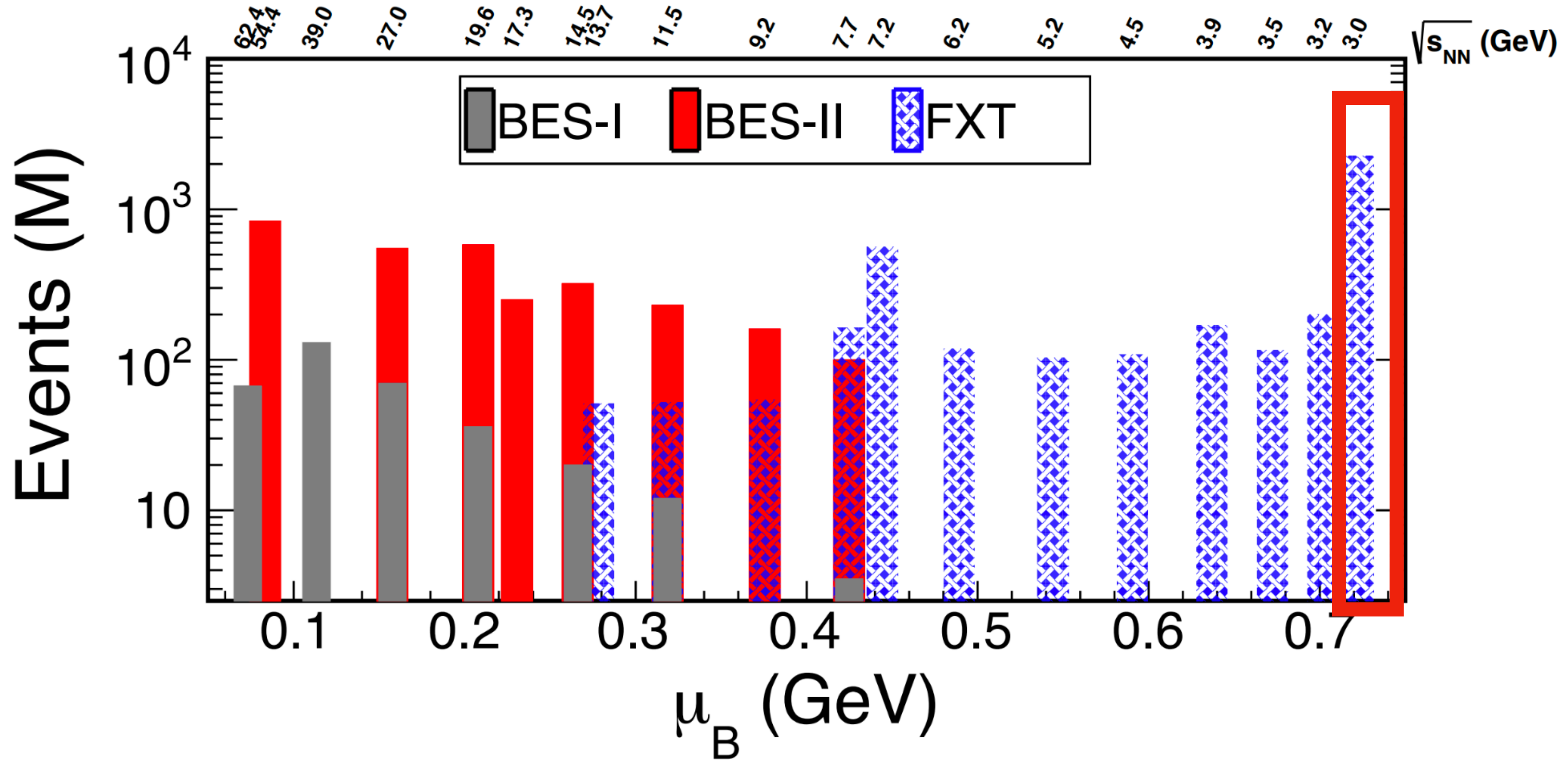

- Precision measurements on hypernuclei properties
- Energy dependence study of hypernuclei yields
- Search for double Λ hypernuclei
  - e.g. ${}^{4}_{\Lambda\Lambda}\mathrm{He} \rightarrow {}^{4}_{\Lambda}\mathrm{He}\pi$, ${}^{5}_{\Lambda\Lambda}\mathrm{He} \rightarrow {}^{5}_{\Lambda}\mathrm{He}\pi$

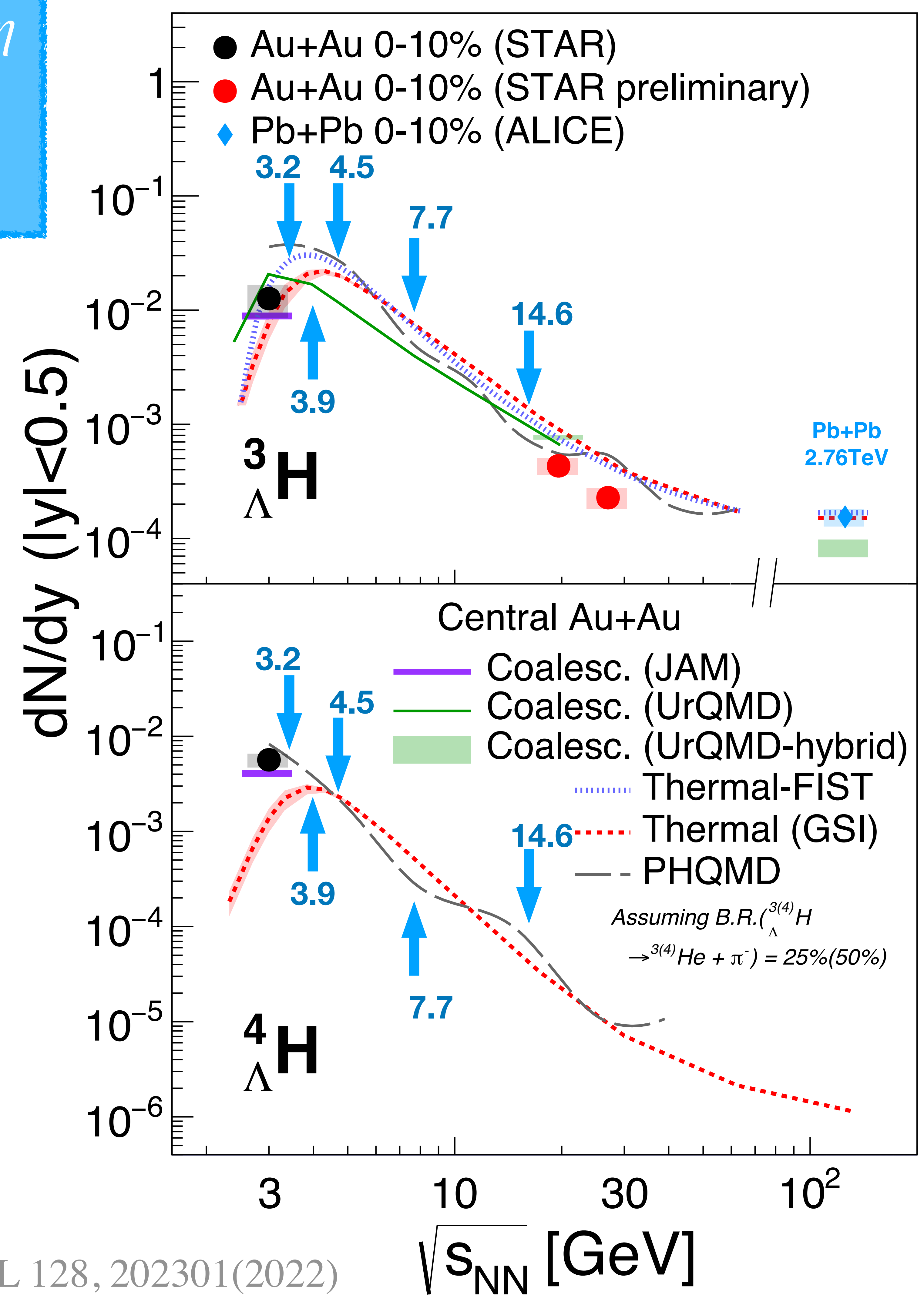

STAR, PRL 128, 202301(2022)

Outlook

1. iTPC and eToF fully installed in 2019 → extend η acceptance and improve PID at large η
2. High statistics data in STAR BES-II $\sqrt{s_{NN}}$ = 3.0 - 54.4 GeV, especially the **2 billion events** collected at 3 GeV in 2021 → larger statistics, higher precision

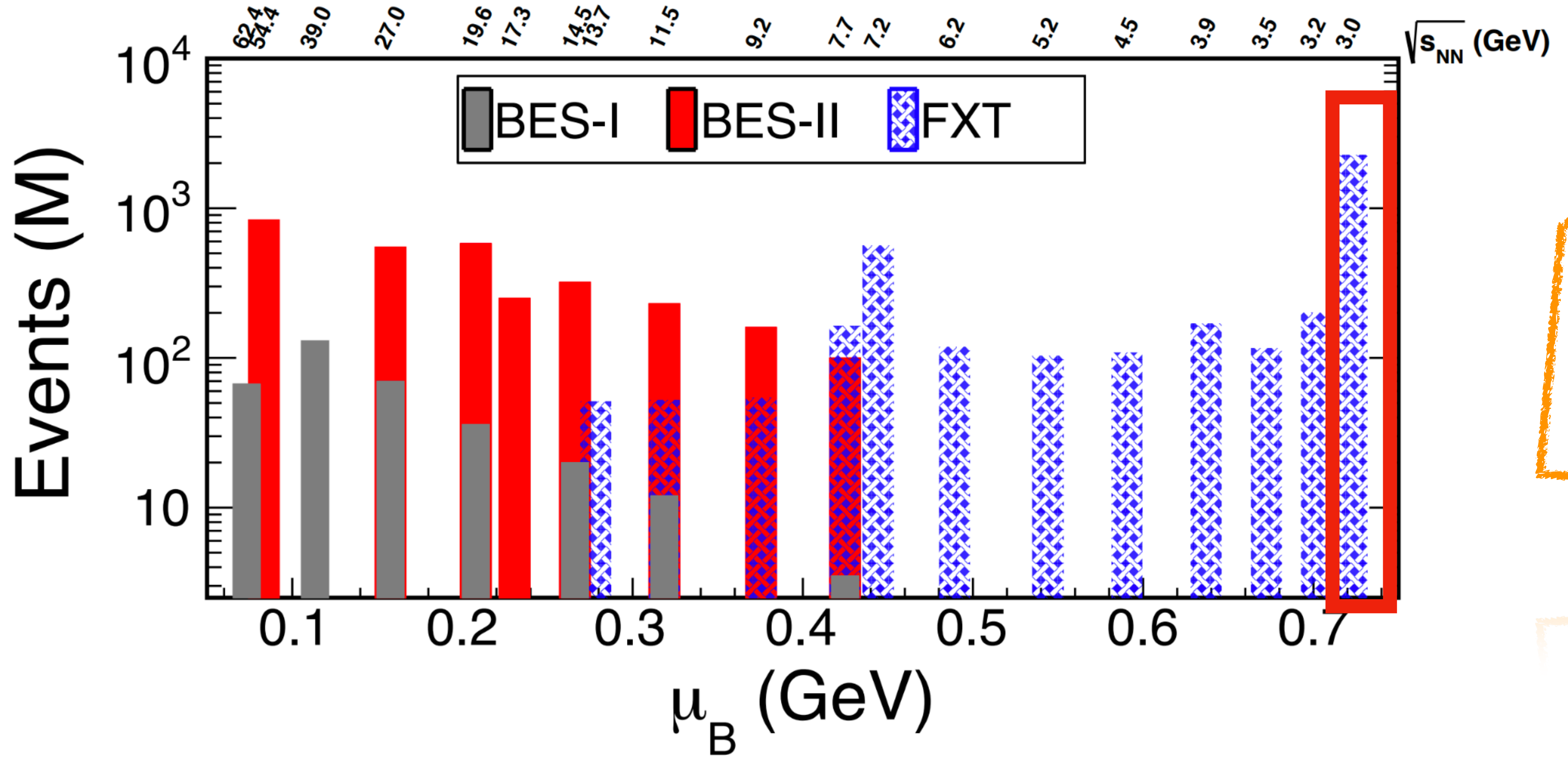

Thank you!

- Precision measurements on hypernuclei properties
- Energy dependence study of hypernuclei yields
- Search for double Λ hypernuclei
  - e.g. ${}^{4}_{\Lambda\Lambda}\mathrm{He} \rightarrow {}^{4}_{\Lambda}\mathrm{He}\pi$, ${}^{5}_{\Lambda\Lambda}\mathrm{He} \rightarrow {}^{5}_{\Lambda}\mathrm{He}\pi$

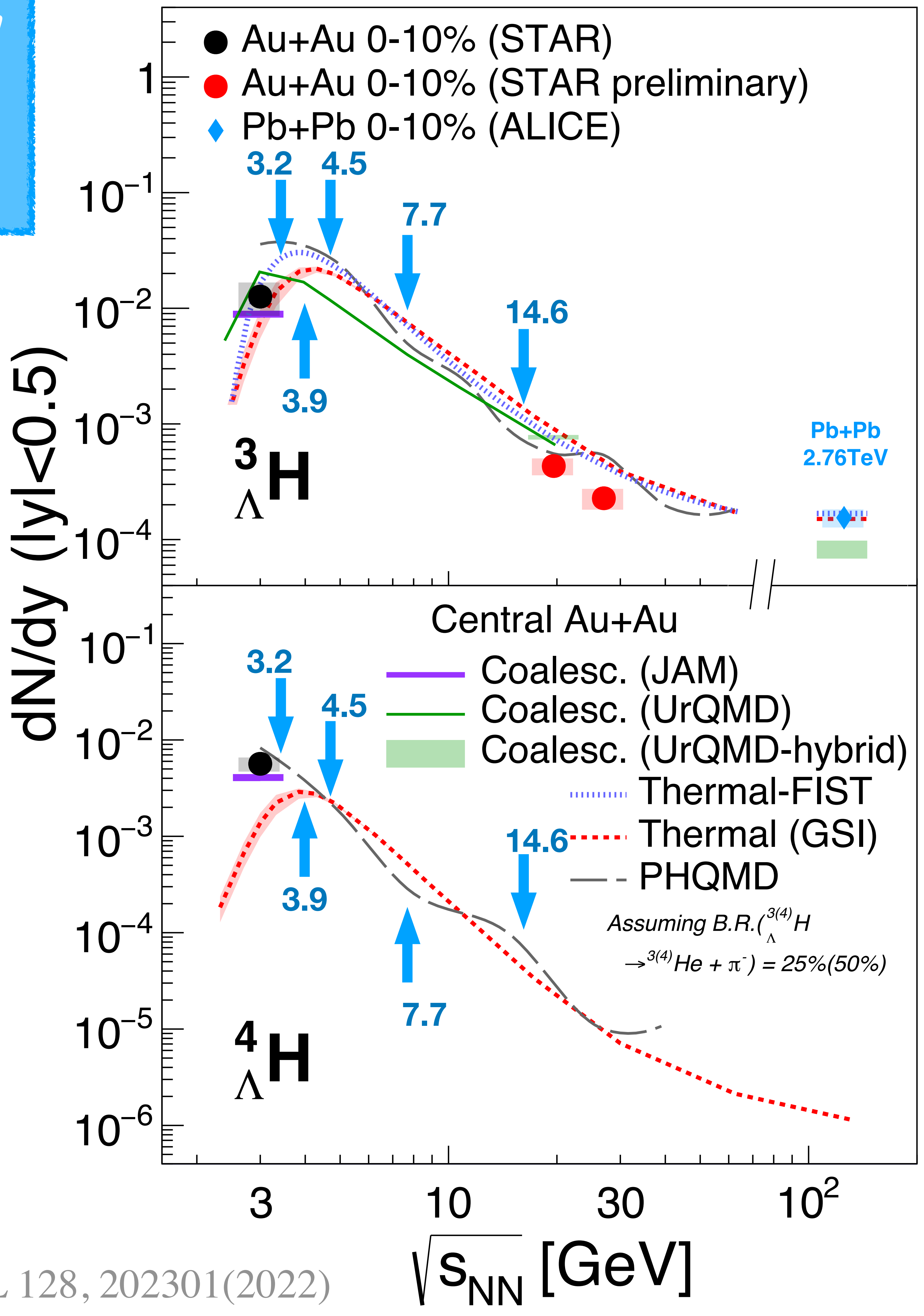

STAR, PRL 128, 202301(2022)

Backups

Model parameters

- Coalescence takes place if the spatial coordinates and relative momenta of constituents are within a sphere of radius (Δr, Δp)
  - JAM + coalescence:

	Δr [fm]	Δp [GeV/c]
d	4.5	0.3
t	4	0.3
$^{3}_{\Lambda}$H	4	0.12
$^{4}_{\Lambda}$H	4	0.3

  - UrQMD cascade + coalescence in slide 14:

	Δr [fm]	Δp [GeV/c]
d	3.7	0.3
t/^{3}He	3.3	0.3
^{4}He	3.4	0.3
$^{3}_{\Lambda}$H	4	0.15
$^{4}_{\Lambda}$H	4	0.25

  - UrQMD+ coalescence in slide 16:

	Δr [fm]	Δp [GeV/c]
NN	3.575	0.285
(NNΛ)a	9.5	0.135
(NNΛ)b	4.3	0.25

- Assuming two parameter sets (a) and (b) for $^{3}_{\Lambda}$H.
  - (a) Δr = 9.5 fm, similar to $^{3}_{\Lambda}$H size.
  - (b) Δr = 4.3 fm, similar to triton size.
- $\sqrt{s_{NN}} \leq$ 20 GeV, UrQMD cascade + coalescence; $\sqrt{s_{NN}} \geq$ 20 GeV, UrQMD hybrid + coalescence; Δp djusted to match each other at 20 GeV.

${}^{3}_{\Lambda}H$ 3-body signal

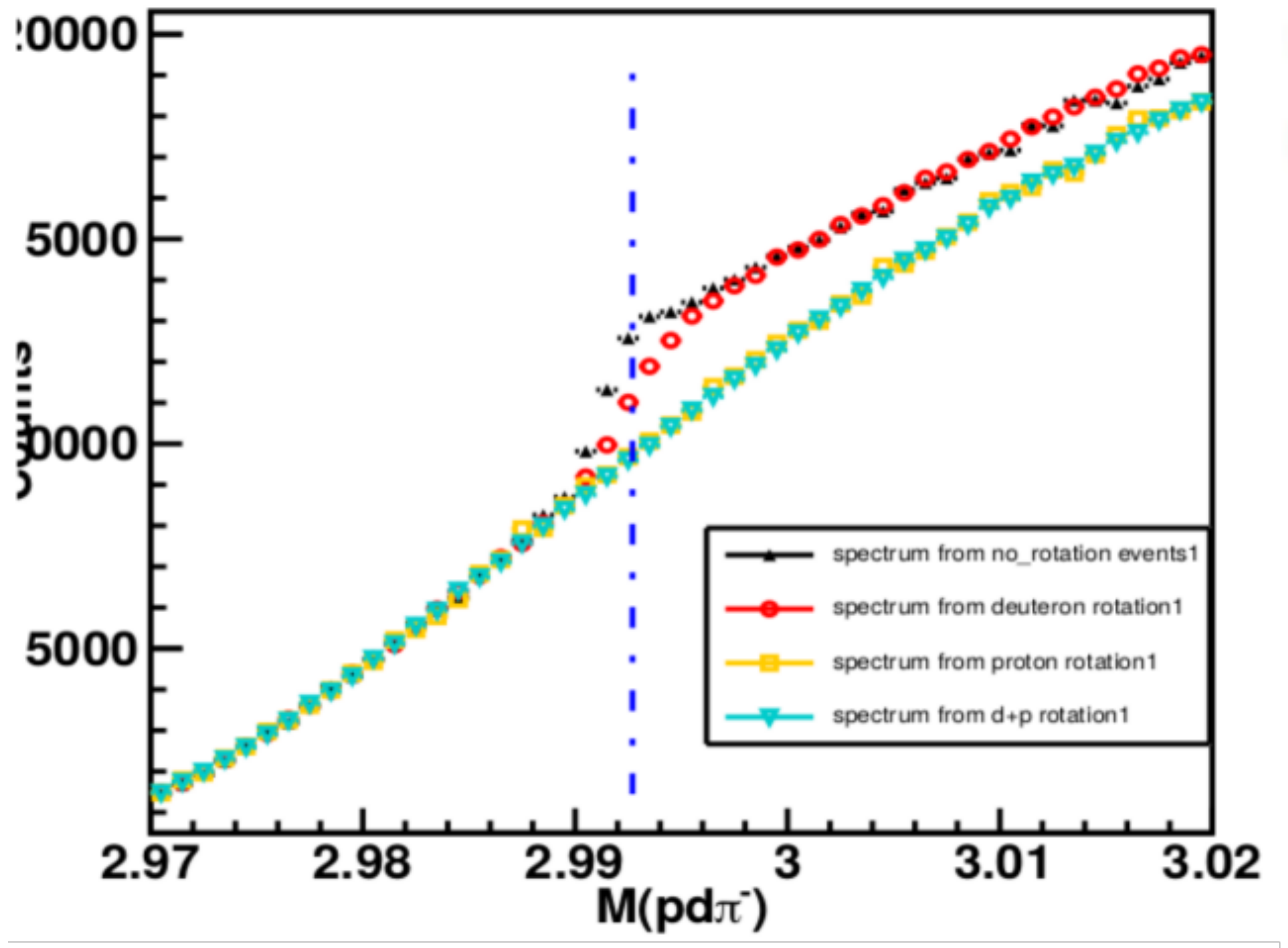

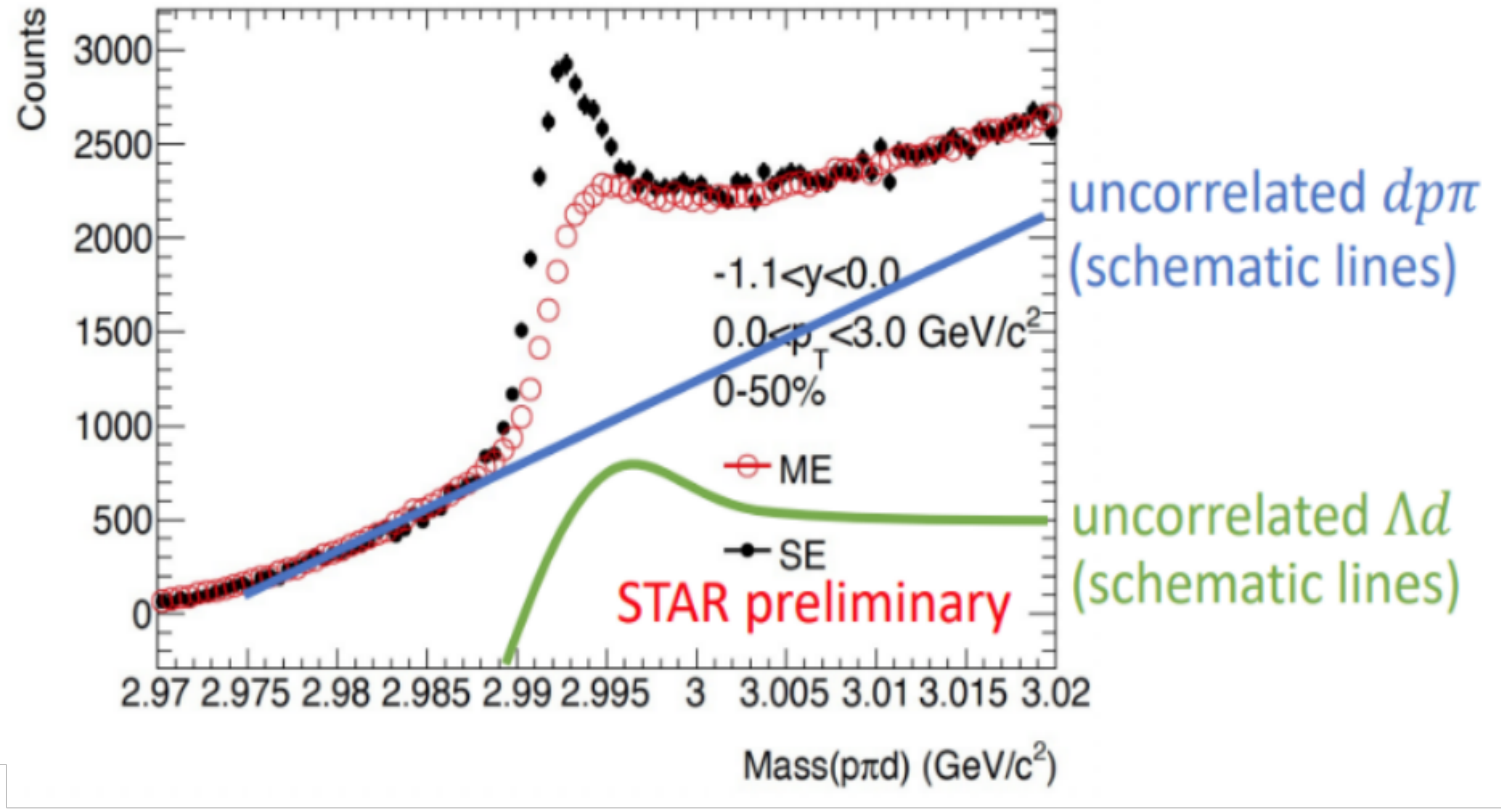

If rotate proton or pi-(d+p） , it can not well describe the data mass.

${}^{3}_{\Lambda}H$ Λ-binding energy

- Recent results:
  - STAR 2020(Nature Phys. 16 (2020) 409):
    - B_{Λ} = 410 ± 120(stat.) ± 110(syst.) keV
    - World average: 181 ± 48 keV
  - ALICE 2021(arXiv:2209.07360, 2022):
    - B_{Λ} = 72 ± 63(stat.) ± 36(syst.) keV
    - World average(PLB 837 (2023)137639): 148 ± 40 keV

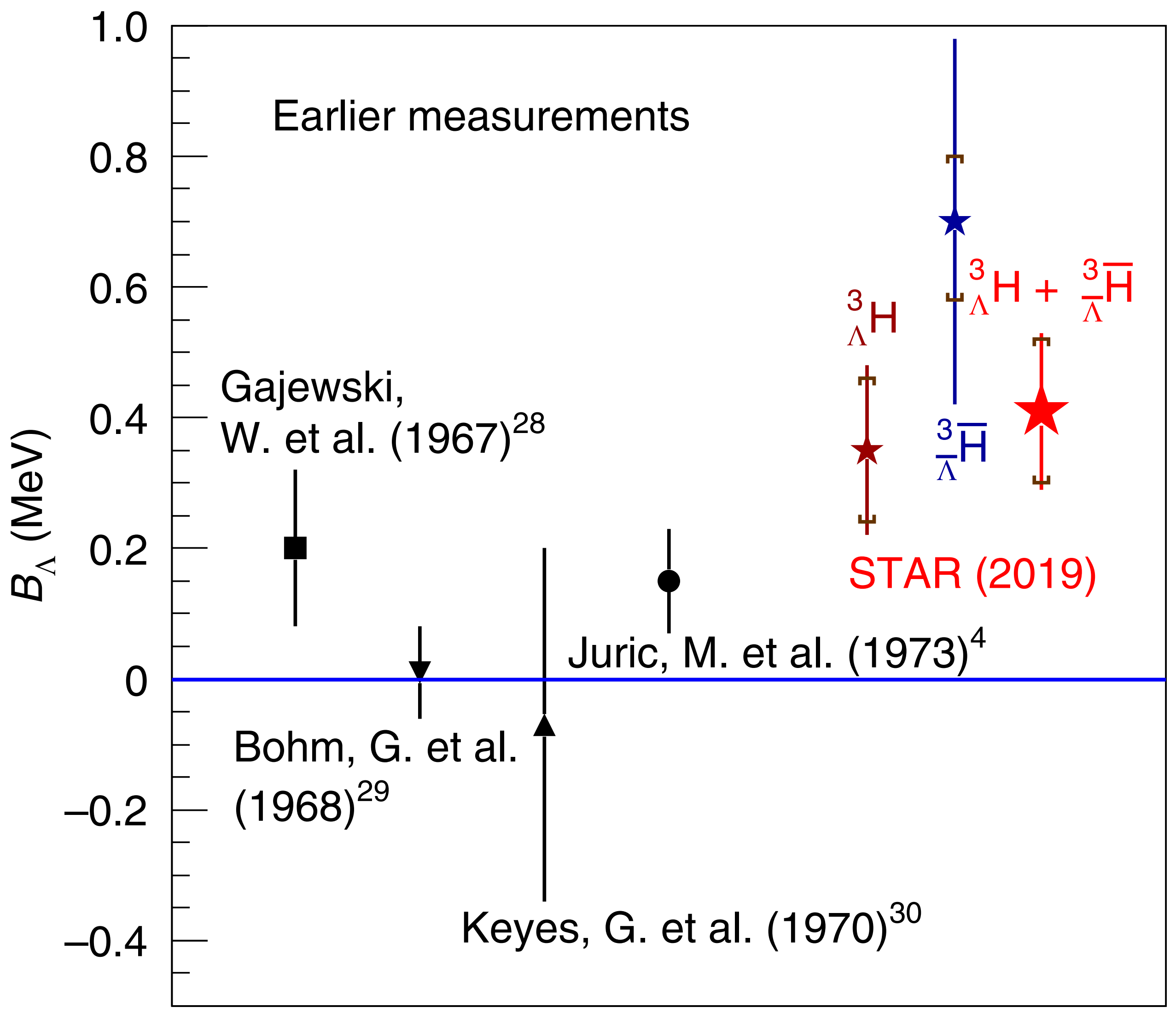

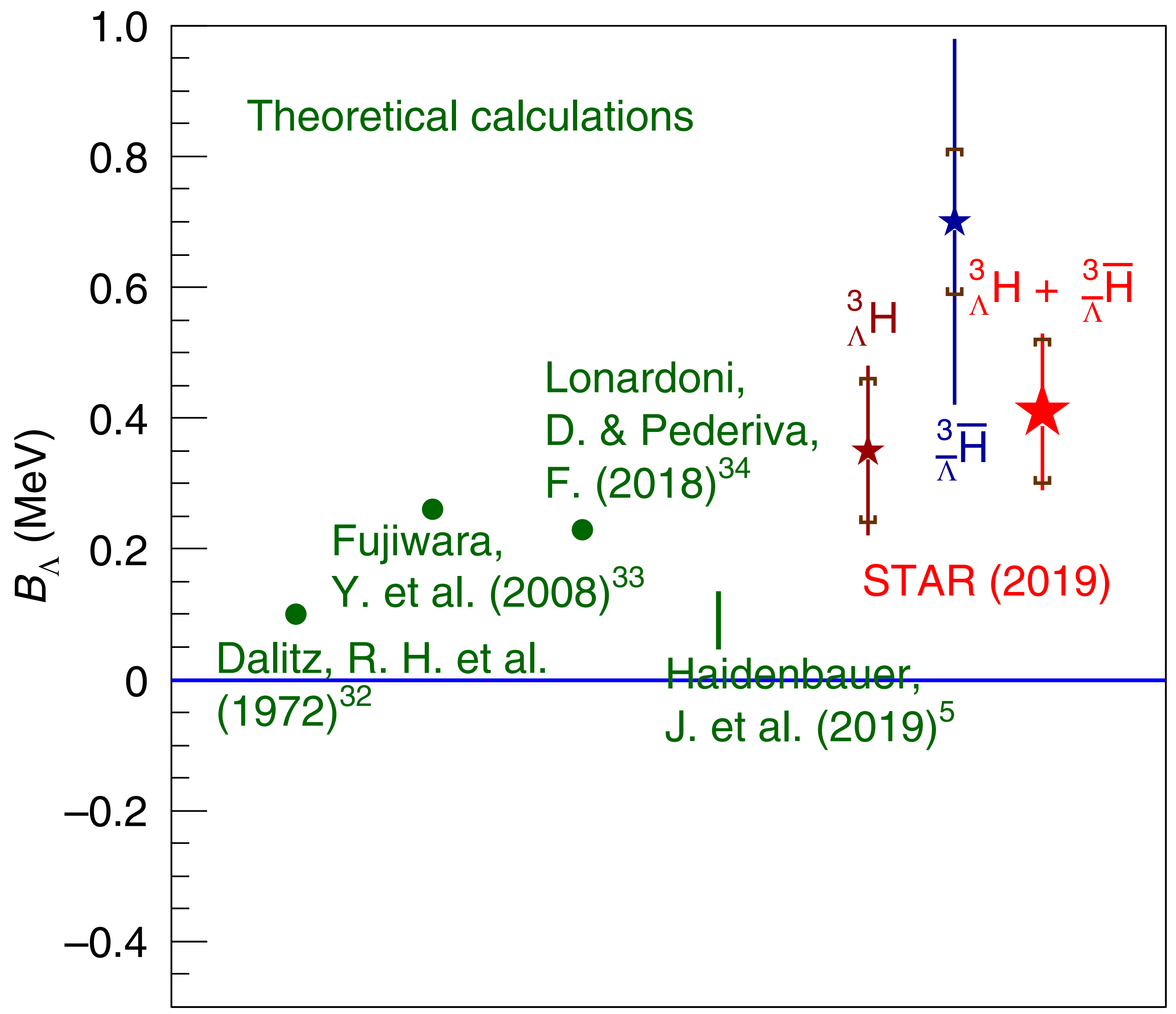

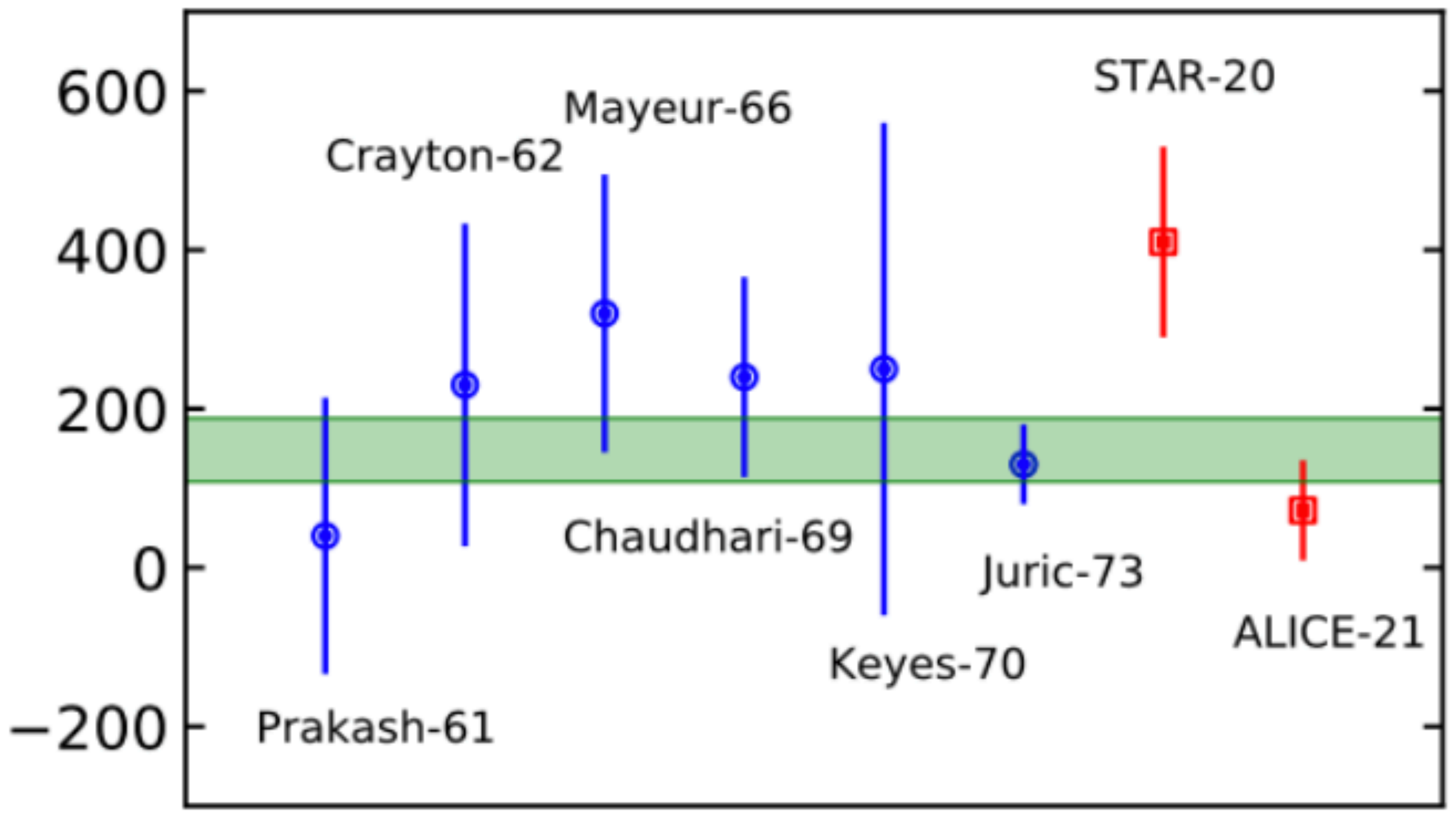

Lifetime

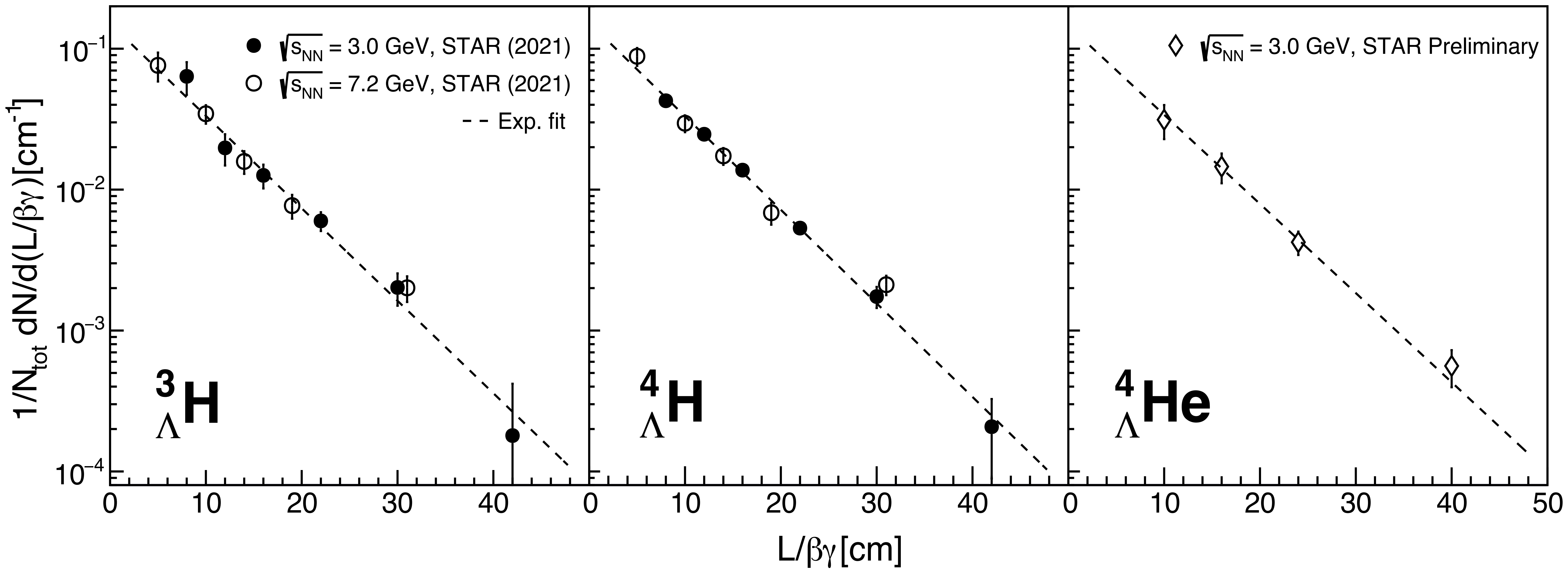

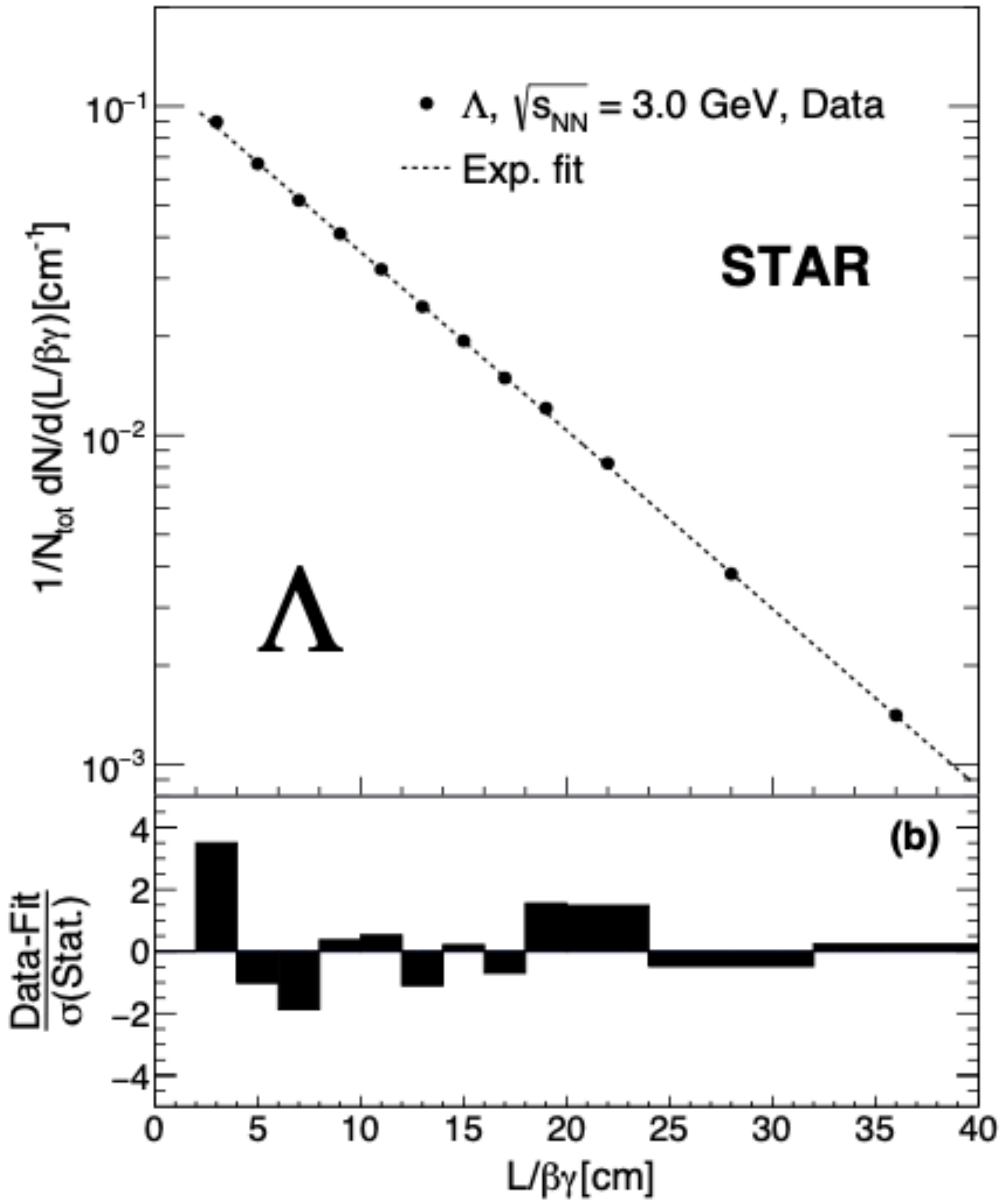

- Lifetime τ extracted via $\mathrm{N(t) = N_0 e^{-L/\beta\gamma c\tau}}$
- Λ lifetime cross check : 267±4 ps, consistent with PDG value (263±2 ps)
- $^{3}_{\Lambda}\mathrm{H}$ and $^{4}_{\Lambda}\mathrm{H}$ lifetimes from 3.0 GeV consistent with 7.2 GeV results